

Research Progress of Multicomponent and Multilevel 3D Printing Materials

ZHANG Qiang*, SHI Yan, GAO Cunfa

State Key Laboratory of Mechanics and Control for Aerospace Structures, Nanjing University of Aeronautics and Astronautics, Nanjing 210016, P. R. China

(Received 1 June 2023; revised 11 September 2023; accepted 20 October 2023)

Abstract: Multicomponent and multilevel 3D printing materials (McMI3DPMs) are an emerging class of advanced materials stemming from the convergence of cellular materials, composites, and additive manufacturing. Since their additive manufacturing-derived 3D architectures span a wide range of composition and structural levels, McMI3DPMs are conferred with outstanding mechanical properties that are often considered to be mutually exclusive (e.g., high strength and high toughness). The scientific challenges that have to be addressed to realize high-performance McMI3DPMs for structural applications are highlighted, and examples of recent research efforts to tackle them are presented. These are reviewed from three aspects: Structural design, manufacturing process modeling, and defect characterization and property evaluation. Finally, we point out the shortcomings of the current research and identify the future development of McMI3DPMs, including discussing several possible directions to further advance the development of the emerging field.

Key words: multicomponent and multilevel 3D printing materials; structural design; manufacturing process modeling; defect characterization and property evaluation

CLC number: O341 **Document code:** A **Article ID:** 1005-1120(2024)01-0001-34

0 Introduction

Multicomponent and multilevel 3D printing materials (McMI3DPMs) are an emerging class of advanced materials with outstanding mechanical properties including light weight, high strength, and superior damage tolerance as well as various practical functionalities including sensing, actuation, and shape reconfiguration, etc^[1-4]. McMI3DPMs stem from the convergence of cellular materials (including lattice materials), composite materials, and additive manufacturing (or more commonly known as 3D printing). Therefore, McMI3DPMs naturally inherit the original features of cellular materials and composite materials, and, more importantly, they gain tremendous advantages derived from 3D printing. In particular, the ability of 3D printing to depos-

it distinct phases or constituents in three dimensions in a free form and bottom-up manner enables McMI3DPMs with arbitrary geometric configuration or structure at various length scales, resulting in unprecedented macroscale mechanical properties. With increasing complexity of control over both the resolution and property of composition by 3D printing^[5], the extent of customization to which McMI3DPMs are conferred is continuously increasing. In this sense, McMI3DPMs promise to become architected matter that can easily break the strength-toughness inversion and simultaneously deliver ultralight performance^[6], showing bright prospect in aerospace, automobile, biomedicine, electronics, and many other fields. For example, by manipulating the orientation of short fibers to align in a way of Bouligand (a helicoidal fiber-reinforced structure

*Corresponding author, E-mail address: qiang.zhang@nuaa.edu.cn.

How to cite this article: ZHANG Qiang, SHI Yan, GAO Cunfa. Research progress of multicomponent and multilevel 3D printing materials[J]. Transactions of Nanjing University of Aeronautics and Astronautics, 2024, 41(1):1-34.

<http://dx.doi.org/10.16356/j.1005-1120.2024.01.001>

widely found in a variety of biological materials) within the matrix during the printing process, the damage-resistant properties of the resulting fiber-reinforced composites (FRCs) can be substantially enhanced and may thereby facilitate the development of the next generation of civil aircraft^[7].

Because of their significant application prospects, McMI3DPMs created mainly for structural applications have attracted increasing attention in recent years^[8], and the number of papers and citations published in high-level international academic journals has been growing exponentially. Currently, there exist two major scientific challenges that hinder the development of McMI3DPMs with desirable mechanical performance:

(1) One is through what kind of structural design strategies, including new design concepts, accurate theories and algorithms, can effectively improve material properties of interest. In order to design materials with outstanding mechanical properties, it is necessary to follow some basic mechanics principles to tell which design patterns contribute to enhancing properties. There are varieties of animals and plants in nature, and some of the materials that make up the bodies of these animals and plants have evolved excellent mechanical performance over millions of years. One can always look into these materials to seek to extract the underlying mechanics principles that govern their remarkable properties. However, not all of the mechanics principles that might be useful for man-made structural materials can be easily found, as some of them may be deeply hidden behind complex 3D architectures spanning multiple lengths or components. This presents challenges for new design concepts of McMI3DPMs. Further, due to the complexity of 3D architectures inspired by biological template materials, it is rather difficult to develop multiscale modeling methods that can provide accurate design guidelines (based on the predicted structure-property relations) while avoiding expensive computational costs.

(2) The other is related to the prediction of material properties, including performance deteriora-

tion, rupture and failure behaviors. The material forming process during the 3D printing process involves a number of complex physical phenomena (such as light irradiation, thermal conduction, species diffusion, phase transition, etc.). In the process of layer-by-layer stacking, the action histories of the physical fields related to these phenomena vary greatly in different regions, resulting in the processing histories of materials in different regions. These processing differences can further couple with the nonlinear behavior of components, leading to various intractable problems such as heterogeneity, anisotropy, and defects (e.g., residual stresses, geometric distortions, and microvoids). As a result, the final performance of McMI3DPMs will deviate from the design and degrade before entering service. Although we can incorporate as many physical phenomena as possible into computational models in pursuit of high fidelity simulations, such models are too expensive in time and too idealistic, lacking the ability to account for defects or accurately predict the properties of materials containing manufacturing defects.

In recent years, researchers have made great efforts to address the above two challenges. In this work, we first review the advances in the development of McMI3DPMs from three closely-related aspects: Design, manufacturing, and property evaluation (Fig.1). Then we prospect the future development of McMI3DPMs and discuss several key research directions in this emerging area from a mechanical point of view. Since there are already some excellent reviews of various functional McMI3DPMs and their applications in areas such as electronics^[9-10], soft robotics^[11-12], and energy storage^[13], in this review, we will only focus on McMI3DPMs which are mainly used for structural applications. The main thread of the review (structure-process-property) reflects the prominent feature of these McMI3DPMs, namely that superior performance is determined by the underlying intricate structure and the advanced manufacturing that enables this structure possible.

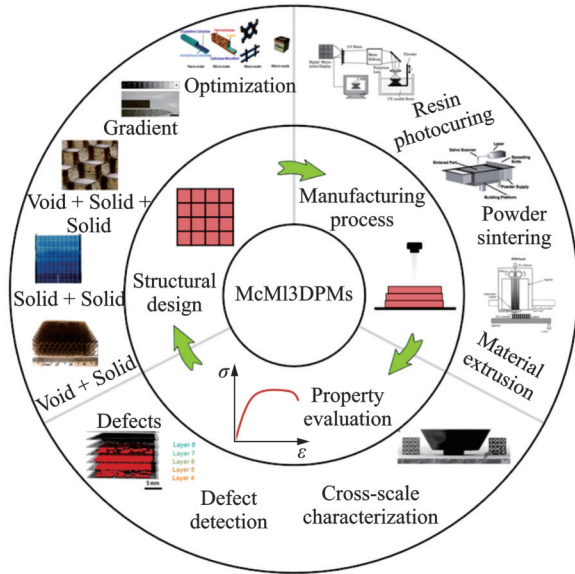


Fig.1 Schematic of three aspects of McMI3DPMs: Structural design, manufacturing process, and property evaluation. Adapted with permission from Ref.[14]. Copyright © 2011, American Association for the Advancement of Science. Adapted with permission from Ref.[15]. Copyright © 2013 WILEY-VCH Verlag GmbH & Co. KGaA, Weinheim. Adapted with permission from Ref.[16]. © 2014 WILEY-VCH Verlag GmbH & Co. KGaA, Weinheim. Adapted with permission from Ref.[17]. Copyright © 2022, The Authors. Adapted with permission from Ref.[18]. © 2017 Elsevier Ltd. Adapted with permission from Ref.[19]. Copyright © 2005 Elsevier B.V. Adapted with permission from Ref.[20]. Copyright © 2007 Published by Elsevier Ltd. Adapted with permission from Ref.[21]. Copyright © 2001 Elsevier Science Ltd. Adapted with permission from Ref.[22]. © 2017 Elsevier B.V. Adapted with permission from Ref.[23]

1 Design Concepts, Structural Types, and Optimization Analysis

Design concept is the core to create McMI3DPMs, but where does the advanced design concept come from? The answer lies in nature. Nature has a wealth of colorful biological materials that can be rather complex in their three-dimensional configurations, giving them the ability to survive in extreme environments. By exploring the structure-property relations of closely observed examples (such as wood, bone, nacre, and teeth) in human's

surrounding, researchers have extracted many fundamental mechanics principles for developing novel concepts to design McMI3DPMs. If we simply classify the obtained McMI3DPMs derived from nature according to the number of components and the presence or absence of void phases (an important means for achieving light weight), we may have the following four types of McMI3DPMs: (1) Two-component ordered structures with one phase as void and the other as a solid; (2) two-component ordered structures with both phases as solids; (3) three-component ordered structures with one phase as void and the other two as solids; (4) multi-component ordered structures with gradient phases. In order to find the optimized topology of these McMI3DPMs, optimization methods based on analytic, numerical, and intelligent algorithms have been pursued and developed. In this section, we review the recent progress in design concepts, structural types, and optimization analysis of McMI3DPMs.

1.1 Two-component ordered structures: One phase as void and the other as a solid

This class of McMI3DPMs can find their templates from biological cellular materials, such as luffa fibers and glass sponge skeletons, where a network of slender struts is used to support loads at low density. When applying this principle to the design of synthetic McMI3DPMs, the network should be engineered to be static and kinematically-determined, which ensures that the deformation of the final material is stretching-dominated rather than bending-dominated^[24]. Since in a truss cellular material, a structure that allows each truss to bear axial forces when subjected to external loads results in high stiffness and strength for a given weight. Another useful mechanics principle learned from nature is that materials become insensitive to flaws at nanoscale^[25]. This size-dependent effect means that when the characteristic size of an engineered structure is nanoscale, the strength of the component that makes up the material is optimized to its theoretical strength, regardless of crack-like flaws.

By exploiting the structural advantages of stretching-dominated constructions and gaining en-

hanced material strength due to size effects, researchers have recently introduced some ultralow density McMI3DPMs with periodic 3D architectures. However, due to the limitations of printing technology, initially, researchers were unable to directly print non-polymer ordered structures with nanoscale trusses, and instead proposed an indirect manufacturing route. For example, Schaedler et al.^[14] built a template by self-propagating photopolymer waveguide prototyping, and then coated the template by electroless nickel followed by etch removal of the template. The resulting nickel microlattices they obtained exhibit densities larger than 0.9 mg/cm^3 , complete recovery after compression exceeding 50% strain, and energy absorption similar to elastomers. These remarkable properties are attributed to structural hierarchy at the nanometer, micrometer, and millimeter scales, in particular the hollow walls with a few hundred nanometers thickness, which allow the bulk material to undergo large effective compressive strains through extensive rotations about node ligaments with negligible strain in the solid nickel component (Fig.2(a), top row). Similar design concepts have been extended to create high-strength, recoverable ceramic nanostructures^[26-27] and ultralight, ultrastiff mechanical metamaterials^[28]. In order to further enhance the mechanical properties, the approach to add another level of hierarchy into original simple periodic nanolattices is utilized by Meza et al.^[29] and Zheng et al.^[30] to enable more efficient load transfer, and suppress global failure. As shown in Fig.2(a)(bottom row), the hierarchical metallic metamaterial has three-dimensional features spanning seven orders of magnitude, from nanometers to centimetres^[30]. At the macroscale, the material achieves high tensile elasticity ($>20\%$) which is not found in its brittle-like metallic constituents, and a near-constant specific strength. With the development of manufacturing techniques, hollow tubes are later replaced with nanoscale trusses to enable 3D nano-architected metals^[31] and carbons^[32]. For example, Vyatskikh et al.^[31] firstly synthesized hybrid organic-inorganic materials that contain Ni clusters to produce a metal-rich photoresist, then used two-photon lithography to sculpt 3D polymer

scaffolds, and pyrolyzed them to volatilize the organics, which produced a $>90\%$ (in weight) Ni-containing architecture (Fig.2(b)).

One of the main limitations of hollow tube- or truss-based network structures is that they cannot achieve the theoretical limit of isotropic elastic stiffness. By using finite-element models, supported by analytical methods and a heuristic optimization scheme, Berger et al.^[33] identified a new material geometry that achieves the Hashin-Shtrikman upper bounds on isotropic elastic stiffness. They found that stiff but well-distributed networks of plates are required to transfer loads efficiently between neighbouring members. The resulting low-density mechanical metamaterials show many advantages including large crushing strains with high energy absorption and high thermal insulation. Soon after, Tancogne-Dejean et al.^[34] identified a full family of elastically isotropic plate-lattices that provide near-optimal mass-specific stiffness, as shown in Fig.2(c). The novel architectures they revealed provide not only high isotropic stiffness, but also a nearly isotropic plastic response. Along this path, many other researchers have also made their respective contributions^[35-36]. However, these structures are problematic from a manufacturing point-of-view, as their closed-cell nature prevents the use of liquid-bath or powder-bed based techniques^[37].

Another limitation of strut-based structures (as well as plate-based structures) is that during manufacturing and loading, stresses become concentrated and defects may occur around the connections^[27]. This is because strut-based structures have a complicated geometry, particularly near the connections between the strut elements. In order to tackle this problem, Han et al.^[38] proposed a structural design pattern where the cells are composed of a single, continuous, smooth-curved shell. In nature, similar geometries can be found on the surfaces of surfactant-water systems, urchin plates, and silicate mesophases, etc. Such surfaces, as pointed out by the researchers^[38], usually exist as interfaces separating two sub-volumes, not as load-bearing shell structures, and a typical example of such a surface is the triply periodic minimal surface (TPMS). The intro-

duction of the new type of ultralow density material composed of a continuous thin shell instead of hollow trusses has quickly attracted attention in the field. Subsequently, Bonatti et al.^[37,39] have systematically studied the structural design methods and mechanical behaviors (such as stiffness, yield strength and energy absorption capability) of the TPMS-based metamaterials. As shown in Fig.2(d) (left), they presented three families of shell-lattices derived from simple-cubic (SC), face-centered cubic (FCC), and body-centered cubic (BCC) tube-lattices using a parameterized surface-smoothing functional. By finite element simulations, they found that the TPMS-like structures of SC, FCC and BCC symmetry exhibited a highly anisotropic mechanical response, both at small and large strains. Apart from TPMS, spinodal shell topolo-

gy, a bi-continuous topology separated by a surface with nearly uniform negative Gaussian curvature and nearly zero mean curvature, is another topology that can be adopted for constructing shell-based architected materials. Compared with periodic designs, the stochastic nature of the topology provides decreased imperfection sensitivity as well as fully isotropic behavior, while still offering near-uniform strain distribution upon loading^[40]. In addition, it has been experimentally demonstrated that the unique shell spinodal topological feature imparts the resulting material with good strength and stiffness: At low relative densities, the strength and stiffness of shell spinodal models outperform those of most lattice materials and approach theoretical bounds for isotropic cellular materials^[41]. Very recently, Senhoro et al.^[42] demonstrated that by locally varying the

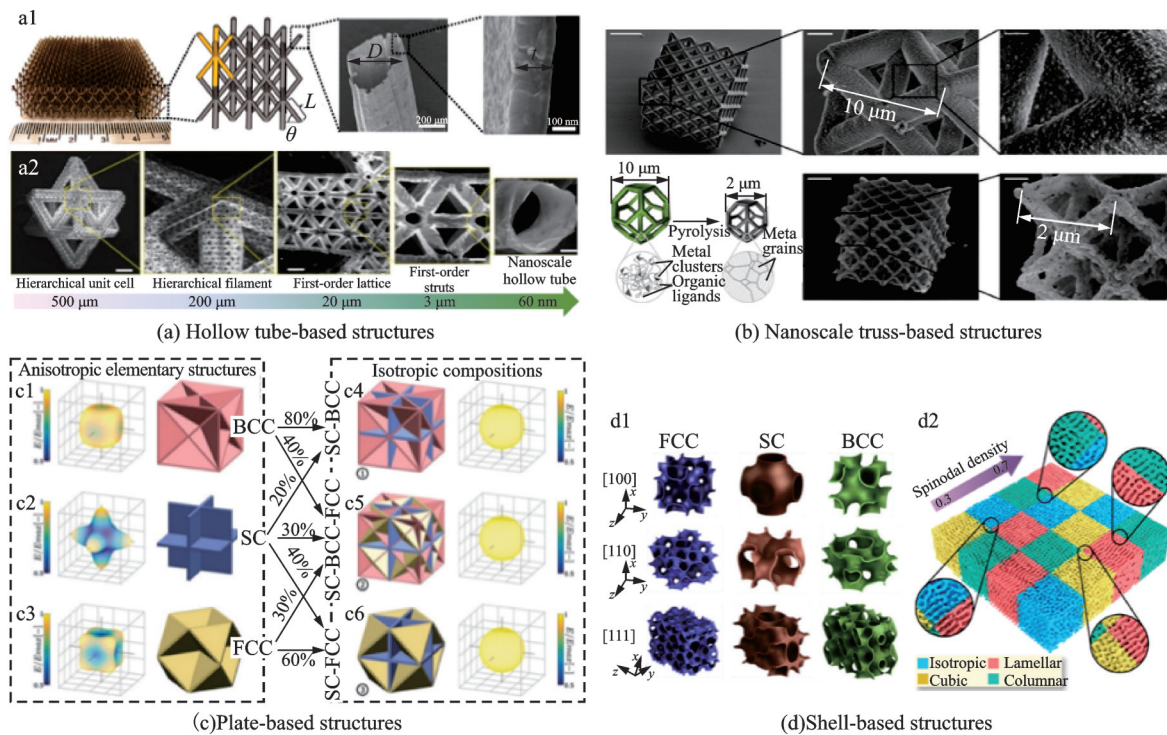


Fig.2 (a) Hollow beam-based structures: (a1) Ultralight metallic microlattices (Adapted with permission from Ref.[14]. Copyright © 2011, American Association for the Advancement of Science), and (a2) multiscale metallic metamaterials (Adapted with permission from Ref.[30]. Copyright © 2016, Springer Nature Limited). (b) Nanotruss-based structures: 3D nano-architected metals (Adapted with permission from Ref.[31]. Copyright © 2018, The Authors). (c) Plate-based structures: Anisotropic elementary structures and isotropic plate-lattice compositions obtained by mixing the elementary structures (Reprinted with permission from Ref.[34]. © 2018 WILEY-VCH Verlag GmbH & Co. KGaA, Weinheim). (d) Shell-based structures: (d1) FCC, SC and BCC TPMS shell-lattices (Adapted with permission from Ref.[39]. © 2018 Acta Materialia Inc. Published by Elsevier Ltd.), and (d2) architected matter obtained by tiling four spinodal architected materials with seamless transitions (Adapted with permission from Ref.[42]. © 2022 The Authors. Advanced Materials published by Wiley-VCH GmbH)

spinodal class (isotropic, lamellar, cubic, and columnar), orientation, and porosity during topology optimization, a large portion of the anisotropic material space can be exploited such that material is efficiently placed along principal stress trajectories at the microscale. In contrast to laminated composites or periodic structured materials, the seamless transition between the four spinodal classes enables a wide design space of architected materials, and the access to direct manufacturing without special treatment at the transitions (Fig.2(d), right).

1.2 Two-component ordered structures: Both phases as solids

Natural materials such as nacre, bone, and the dactyl club are nanocomposites of proteins and minerals assembled in highly-ordered hierarchical structures that give rise to exceptional strength and toughness. When reproducing the ordered structures of these nanocomposites at the micrometer resolution by additive manufacturing, one can obtain bio-inspired composites with better performance than traditional composites.

Nacreous layer of mollusk shells is considered as a model system for toughened biological composites and has been extensively studied to reveal the toughening mechanisms. In the brick-and-mortar (staggered) structure of nacre (Fig.3(a), first from the left), stiff mineral components absorb the bulk of the externally applied loads, while the organic layers in turn provide toughness and prevent the spread of the cracks into the interior of the structure^[43-44]. Dimas et al.^[15] sought to emulate such staggered structure by using multi-material 3D printing at micrometer resolution. The resulting synthetic composites show superior fracture mechanical properties exhibiting deformation and fracture mechanisms reminiscent of mineralized biological composites (Fig.3(a), second from the left). In Ref.[15], the composites are based on a 2D design and are thus 2D staggered composites. In reality, the staggered microstructure in nacre is close to 3D rather than 2D, and 2D design makes materials less capable of transferring loads. Zhang et al.^[45] therefore proposed two different kinds of 3D staggered com-

posites which have square and hexagonal shaped prisms. For both of the two types of 3D staggered composites, as shown in Fig.3(a) (third from the left), the prisms are distributed so that one prism's tip locates in the middle of adjacent prisms in the longitudinal direction. The 3D staggered composite design is proven to exhibit highly enhanced damping response. Conch shells are also mollusk shells, and are an order of magnitude tougher than nacre shells. However, due to their complex 3D hierarchical cross-lamellar structure, it is difficult to create materials that reproduce the elegant structure of conch shells. Recently, this challenge has been tackled by Gu et al.^[46], who presented a 3D conch shell prototype (Fig.3(a), fourth from the left) that can replicate the crack arresting mechanisms embedded in the natural architecture. The results show that adding the second level of cross-lamellar hierarchy can boost impact performance by 70% and 85% compared with a single-level hierarchy and the stiff constituent, respectively.

Although the nacreous structure imparts the material excellent strength and toughness, it does not protect the mollusks from hammer-like strikes from a smashing predator known as mantis shrimp, while the shrimp itself is able to resist damage from the high-velocity blows. The secret stems from the structure of the endocuticle of the mineralized dactyl club of the shrimp^[47-48], which is characterized by a helicoidal arrangement of mineralized fiber layers (Bouligand structure, Fig.3(b), first from the left). Bouligand structure provides an enhanced fracture toughness by forcing a twisting interface along the direction of the crack front and the crack deflection enforces mode mixity and amplifies the surface area per unit required for crack propagation^[49-50]. When this helicoidal design strategy is applied to fabricate FRCs with high-performance, one can obtain the helicoidal structure by stacking unidirectional layers (plies)^[51]. However, classical lamination techniques may lead to premature interlaminar failure. Additive manufacturing can well solve this problem and enable greater precision over the reinforcing architecture. Martin et al.^[52] presented a 3D magnetic printing method for the fabrication of composites

similar to cholesteric-reinforced dactyl clubs (Fig. 3 (b), second from the left). During the printing process, the orientation of the ceramic reinforcement particles can be finely tuned, thus contributing to excellent mechanical properties. Zaheri et al.^[53] later found that the helicoidal structure in the cuticle of the figeater beetle is not fixed, but changes at different stages of the animal's life cycles to adapt to growth needs. They utilized 3D printing to complement their understanding of the helicoidal architecture as an adaptable material system where the pitch angle between layers of the manufactured helicoidal fibrous systems was changed (Fig. 2(b), third from the left). Results show that the mechanical response of these synthetic composites exhibited elasticity, inelasticity, and failure with a strong dependence on pitch angle. Recently, inspired by the survival war between the mantis shrimps and abalones, Wu et al.^[54] designed a discontinuous fibrous Bouligand (DFB) architecture, a combination of Bouligand and nacreous staggered structures (Fig. 2(b), fourth from the left). Systematic bending experiments for 3D-printed single-edge notched specimens with such architecture indicate that total energy dissipations are insensitive to initial crack orientations and show optimized values at critical pitch angles. Fracture mechanics analyses further demonstrate that the hybrid toughening mechanisms of crack twisting and crack bridging mode enable excellent fracture resistance with crack orientation insensitivity.

In 2D staggered composites, when the fraction of stiff phases is low, the isolated layout of stiff phases leads to a significant reduction in the modulus of the composite. In addition, only when the loading direction is along the length direction of the stiff phase can the toughness be enhanced. These limitations can be avoided by adopting a mesh-like structure, as identified by Libonati et al. in 2016^[55]. Such structure is derived from osteons (Fig. 3(c), first from the left), which are the key microstructural features actively involved in the process of cortical bone fracture. In the 3D-printed mesh-like composites (Fig. 3(c), second from the left), the researchers recognized multiple toughening mecha-

nisms similar to those occurring in bone: On the small scale, there exist fibril bridging occurring in the soft phase, formation of microvoids and microcracks occurring ahead the crack tip, and uncracked-ligament bridging; on the large scale, there exists crack deviation. Lei et al.^[56] subsequently designed a class of 2D elastomer filled composites with periodic units using the concept of mesh-like structure as well (Fig. 3(c), third from the left). Their focus is on the dynamic response and fracture behaviors of the resulting material as well as their dependence on the volume fraction, component properties, and the geometry of the unit cell.

In all of the three kinds of bio-inspired composites discussed above, the reinforcements are discrete, dispersed, and isolated phases embedded in an otherwise homogeneous matrix material, while interpenetrating phase composites (IPCs) are a class of materials in which both phases are continuous^[57]. Natural interpenetrated structures comprised of stiff and soft materials can provide excellent comprehensive performance, including strength, toughness, impact resistance, and energy absorption. Typical examples include sea urchin skeleton and microvascular networks. Wang et al.^[58] designed and printed an IPC composed of glassy polymer and rubbery polymer materials in SC, BCC (Fig. 3(d), left), and FCC Bravais lattices. The model system they studied are based on microstructures which possess interfaces close to those of TPMS. The resulting materials are observed to have enhancements in stiffness, strength and energy dissipation. Later, they experimentally investigated the fracture toughness of another group of 3D printed IPCs with different lattice symmetries^[59]. Results show that crack-bridging, process zone formation, and crack-deflection together contribute to the enhanced fracture toughness. However, due to the periodic nature of TPMS, all of TPMS-based IPCs are generally difficult to manufacture in a scalable fashion, thus limiting their potential applications. Recently, Zhang et al.^[60] designed IPCs with spinodal shell reinforcement (Fig. 3(d), right) and investigated their mechanical properties based on 3D-printed samples. Results show that spinodal shell-based IPCs have

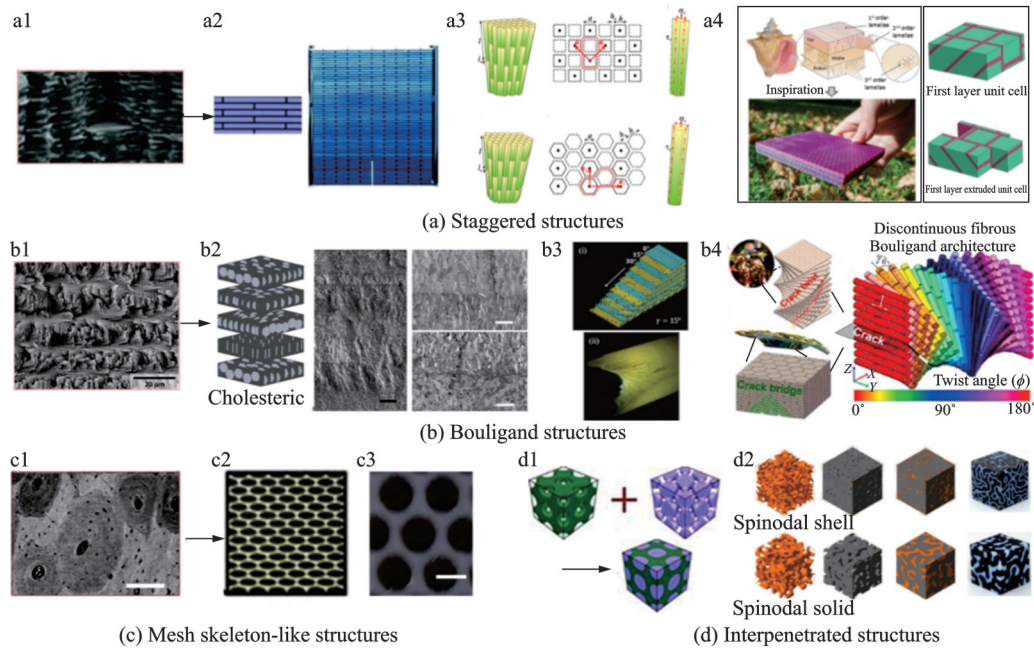


Fig.3 (a) Staggered structures: (a1) Microscopic image of nacre structure, and (a2) nacre-inspired structure design pattern and the printed material (Both (a1) and (a2) are adapted with permission from Ref.[15]. Copyright © 2013 WILEY-VCH Verlag GmbH & Co. KGaA, Weinheim), (a3) 3D staggered composites with square prisms and hexagonal prisms (Reprinted with permission from Ref.[45]. Copyright © 2015 Elsevier Ltd.), and (a4) conch shell-inspired material with three-tier crossed-lamellar structure (Reprinted with permission from Ref.[46]. © 2017 WILEY-VCH Verlag GmbH & Co. KGaA, Weinheim). (b) Bouligand structures: (b1) A cholesteric architecture of mineralized chitin fibres found in the dactyl club of the mantis shrimp (Adapted with permission from Ref.[48]. Copyright © 2014 Acta Materialia Inc. Published by Elsevier Ltd.), (b2) simplified and printed architecture derived from the Bouligand structure (Adapted with permission from Ref.[52]. Copyright © 2015, The Authors), (b3) fractured surfaces in the tested helicoidal composites (Adapted with permission from Ref.[53]. © 2018 WILEY-VCH Verlag GmbH & Co. KGaA, Weinheim), and (b4) structural characteristics in a pitch for a DFB architecture, a combination of Bouligand and nacreous structure (Reprinted with permission from Ref.[54]). (c) Mesh skeleton-like structures: (c1) Microstructure of cortical bone (Adapted with permission from Ref.[52]. Copyright © 2015, The Authors), (c2) bone-inspired material topologies with elliptical inclusions (Adapted with permission from Ref.[55]. © 2016 WILEY-VCH Verlag GmbH & Co. KGaA, Weinheim), and (c3) bone-inspired material topologies with circular inclusions (Adapted with permission from Ref.[56]. © 2018 Elsevier Ltd.). (d) Interpenetrated structures: (d1) 3D periodic co-continuous composites consisting of $2 \times 2 \times 2$ unit cells with body-centered-cubic lattice (Adapted with permission from Ref.[58]. Copyright © 2011 WILEY-VCH Verlag GmbH & Co. KGaA, Weinheim), and (d2) spinodal shell and spinodal solid based interpenetrating phase composites topologies (Adapted with permission from Ref.[60]. © 2021 Elsevier Ltd.)

comparable compressive strength and stiffness to TPMS-based IPCs and octet truss lattice-based IPC, while exhibiting far less catastrophic failure and greater damage resistance.

1.3 Three-component ordered structures: One phase as void and the other two as solids

Lightweight cellular composites are a class of McMI3DPMs that have origins from natural materials with higher mechanical performance and lighter weight. The most ubiquitous example is wood, in

particular balsa, which has a stiffness-to-weight ratio comparable to that of steel along the axial loading direction^[61]. The basic design concept extracted from these biological cellular composites is to use periodic cells to construct ordered microscopic structures while using fibers to reinforce the walls of these cells. Since the concept is straightforward, the challenge is how to control the orientation of the fibers at the cell wall level, and how to simultaneously control the structure and arrangement of the cells.

Compton et al.^[16] first attempted to give one answer in 2014. They used direct-ink writing (DIW) to print (square, hexagonal, and triangular) honeycomb composites with hierarchical structures. During the printing process, fibers with high aspect ratio are aligned along the print path due to the shear stresses generated at the nozzle tip, acting in a role of unidirectional enhancement (Fig.4(a), first). Using print path to control fiber orientation adds an entirely new dimension to engineer design and optimization, where composition, stiffness, and toughness within a bulk 3D object can be digitally integrated with component design to achieve a highly optimized structure. In order to further increase the damage tolerance of FRCs and based on the fact that some natural systems have complex fiber arrangements within continuous matrices, the same research group developed a rotational 3D printing method that controls spatially the orientation of short fibers in polymer matrices solely by varying the nozzle rotation speed relative to the printing speed (Fig.4(a), second). With the developed new method, they designed and fabricated carbon fiber-epoxy composites composed of volume elements with programmably defined fiber arrangements, including those with purely helical fiber orientations akin to natural composites^[62]. Similar methods have also been adopted by Franchin et al.^[63] to fabricate ceramic matrix composite (CMC) structures where complex CMC structures with porosity of about 75% and compressive strength of about 4 MPa are successfully printed (Fig. 4(a), third). Apart from the method to use shear force to control fiber orientation, some researchers have also exploited external fields (such as sound field^[64] and electric field^[65]) to locally tune the fiber orientation during the printing process in order to fabricate complex structured composites. Although carbon fiber reinforced polymer composite has a high stiffness-to-weight ratio, it is not suitable for energy dissipation as failure with very little or no plastic deformation. Recently, Xu et al.^[66] developed a photo-curing-based 3D printing method to create carbon fiber reinforced polymer composites that have not only a high stiffness-to-weight ratio but also good energy dissipation

capabilities. In their method, the used photo sensitive ink is composed of fibers, monomers and crosslinkers. The advantage of this method is that it enables design and fabrication of highly complex 3D microlattices (Fig.4(a), fourth).

Compared with short fiber-reinforced cellular composites, continuous fiber-reinforced cellular composites offer significant improvement in mechanical properties (stiffness and strength) due to better reinforcing effects^[67-68]. For example, Sugiyama et al.^[69] investigated the 3D printing manufacturability of arbitrary core shapes using continuous fiber filament without support materials and successfully fabricated sandwich structures with honeycomb, rhombus, rectangle, and circle core shapes as a single piece, as shown in Fig.4(b) (top). In spite of this, it is difficult to create architected materials that possess both high stiffness and toughness, since these properties are often mutually exclusive. Mueller et al.^[70] came up with a method to overcome this by creating architected lattices composed of core-shell struts where the core is a flexible epoxy, the shell is a brittle epoxy, and the interfacial layer is an elastomeric silicone (Fig.4(b), bottom). They found that the presence of an elastomeric interfacial layer introduces a compliant region between the two epoxy materials within the individual struts. This can reduce the struts' overall stiffness and makes it difficult for the stress to be transferred from the shell to the core, thus contributing to increase toughness.

1.4 Other multi-component ordered structures: Gradient phases

It has long been recognized that the introduction of spatial gradients can effectively improve the mechanical properties of materials by alleviating stress concentrations or singularities^[71]. Indeed, functional gradients are one of the basic structural elements of diverse biological architectures (e.g., squid beak and sponge spicules), and they have evolved to perform their functions efficiently within certain environmental constraints. Therefore, creating gradients provides a promising approach for designing high-performance structural materials. According to Liu et al.^[71], the gradients are fundamen-

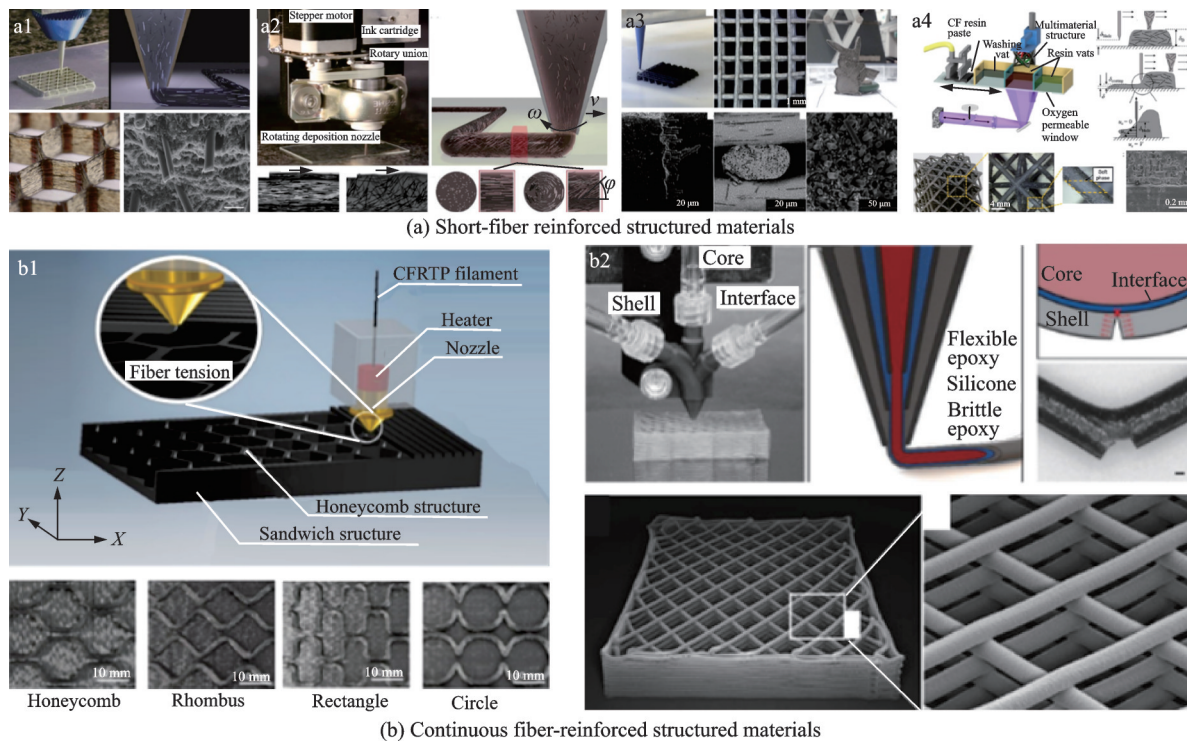


Fig.4 (a) Short-fiber reinforced structured materials: (a1) Lightweight cellular composites printed by progressive alignment of high aspect ratio fillers within the nozzle during composite ink deposition (Adapted with permission from Ref.[16]. © 2014 WILEY-VCH Verlag GmbH & Co. KGaA, Weinheim), (a2) damage-tolerant composites by rotational 3D printing where fiber orientation can be programmed into a helical pattern through the rotating nozzle (Adapted with permission from Ref.[62]), (a3) ceramic matrix composite structures by direct ink writing where the ink contains chopped fibers (Adapted with permission from Ref.[63]. © 2017 The American Ceramic Society), and (a4) two-phase lightweight, stiff and high damping carbon fiber reinforced polymer microlattices by multi-material microstereolithography system (Adapted with permission from Ref.[66]. © 2020 Published by Elsevier B.V.). (b) Continuous fiber reinforced structured materials: (b1) 3D printing of a sandwich structure with continuous carbon fiber composite using fiber tension (Adapted with permission from Ref.[69]. © 2018 Elsevier Ltd.), and (b2) architected lattices with high stiffness and toughness via multicore-shell 3D printing (Adapted with permission from Ref.[70]. © 2018 WILEY-VCH Verlag GmbH & Co. KGaA, Weinheim)

tally associated with the changes in two sorts of ingredients, i.e., chemical compositions/constituents, and structural characteristics (which further involve the arrangement, distribution, dimensions and orientations of structural building units). Although it is promising, it is often quite difficult to create desired gradients through traditional processing technologies. By contrast, additive manufacturing facilitate the realization of various functional gradients and thus gradient-based McMI3DPMs.

Kokkinis et al.^[72] developed a material extrusion-based 3D-printing platform to fabricate elastomer gradients spanning three orders of magnitude in elastic modulus and investigated the role of various bioinspired gradient designs on the local and global

mechanical behavior of synthetic materials. As shown in Fig.5(a) (left), the rectangular polymer film with a small circular silica glass island (used as stress concentrator) embedded in the center is globally stretched at both ends. Four different gradient designs (the nongraded, the ascending gradient, the descending gradient, and the soft layer designs) came up and their effects on the strain distribution around the hard island were compared. Results from digital image correlation show that when stretching the specimens to 25% global engineering strain, the nongraded profile shows strain concentration at the interface between the soft phase and the hard island, while the increasing elastic modulus of the ascending gradient reduces the strain on the material

around the glass island. Digital light processing is a high-resolution fast-speed 3D printing technology suitable for various materials. Cheng et al.^[17] reported a digital light processing-based centrifugal multi-material 3D printing method to generate large-volume heterogeneous 3D objects where composition, property and function were programmable at voxel scale. By increasing the content of hard voxels from 0 to 100%, the modulus of the printed digital material increases from 0.8 MPa to 1 GPa (Fig. 5 (a), right). Fig. 5(a) (right) also presents a printed octet truss structure consisting of four colors where the layers of white, black, light green and transparent units are stacked from bottom, and the units with

four colors are alternatively placed in the top layer.

In addition to changing chemical composition, adjusting structure can also create gradients. Fig. 5 (b) shows two examples. The first example is about architected materials that can be designed to be damage-tolerant by designing the orientation and arrangements of the composed mesoscale structures^[73]. The hardening mechanisms here is analogous to that in crystalline materials where toughness can be achieved through introduction of grain boundaries, precipitates and phases. The second is about graded polymer foams, where the stiffness gradient can be achieved by changing the bubble size and thus the porosity during the printing process^[74]. By

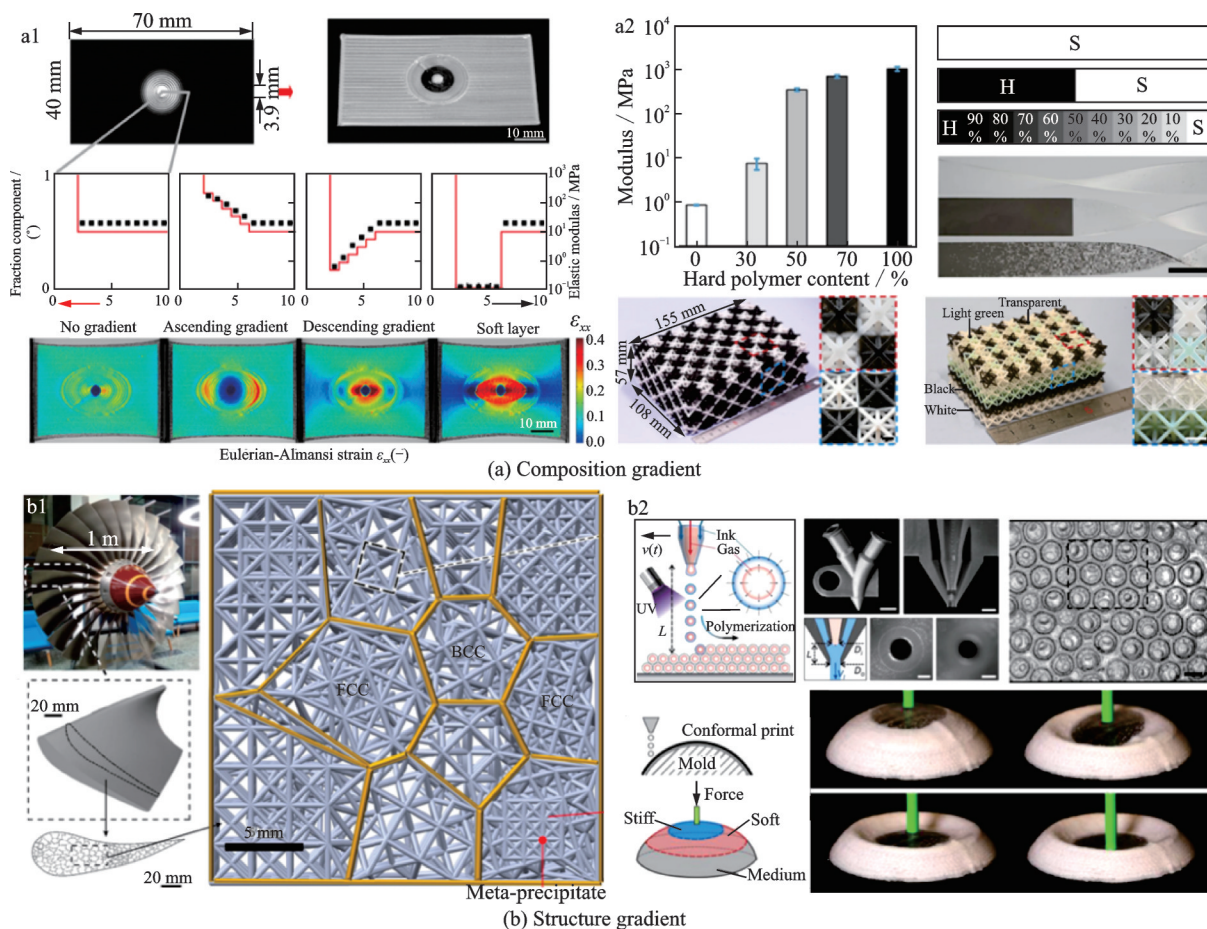


Fig. 5 (a) Composition gradient: (a1) Model system for the investigation of 2D mechanical gradients for joining dissimilar materials (Reprinted with permission from Ref.[72]. © 2018 WILEY-VCH Verlag GmbH & Co. KGaA, Weinheim), and (a2) demonstration of printed specimens exhibiting multiple mechanical properties at different locations in a large volume two-material octet truss (Adapted with permission from Ref.[17]. Copyright © 2022, The Authors). (b) Structure gradient: (b1) Lightweight and damage-tolerant architected materials inspired by crystal microstructure (Adapted with permission from Ref.[73]. Copyright © 2019, Springer Nature Limited), and (b2) schematic illustration and experimental image of bubbles composed of a fluid shell-gas core and mechanical properties of printed polymer foams (Adapted with permission from Ref.[74]. © 2019 WILEY-VCH Verlag GmbH & Co. KGaA, Weinheim)

locally varying the relative density, the polymer foam stiffness is allowed to be tuned over several orders of magnitude. These features can be exploited for conformal printing of a tri-stable cap (with stiff and soft regions), which snaps into different shapes upon continued compression from the top.

1.5 Structural optimization methods

With the design pattern of McMI3DPMs, structural optimization methods have to be adopted to obtain the optimal topology. At present, there are mainly four methods that can be used to optimize structural topology:

(1) Multiscale models. The idea of multiscale modeling of materials has a long history dating back to the mixing rules proposed by Voigt in the 19th century, while the proposed concept of multiscale modeling has emerged over the last few decades and is still steadily evolving. The aim of multiscale mechanics is to identify and quantify relations between various length scales in heterogeneous materials, and the ultimate goal is to extract macroscopic properties of materials from the information occurring at finer scales. Scale bridging is the key in multiscale modeling and the commonly used method for scale bridging is “homogenization”. According to the basis of the underlying problem formulation, the methods of multiscale modeling can be roughly classified into two types: Concurrent methods and hierarchical methods. In concurrent methods, both scales are simultaneously addressed, and different length and time scales can be adopted (in a single domain) and different parts of the domain can be solved with different methodologies. In hierarchical methods, different scales are resolved and coupled in the same part of a domain, and the link between both scales is typically made via averaging theorems or sometimes on the basis of parameter identification only. Readers are suggested to refer to the dedicated reviews^[75-76] for a more detailed discussion of multiscale modeling approaches. Here, we briefly introduce several multiscale models developed for structural optimization of McMI3DPMs. The first example is contributed by Malek et al.^[18], who developed an advanced multiscale model to study the structure-

property relations at different length scales to understand the contribution of the three types of cells (the fibers, rays and vessels) to the remarkable elastic moduli of balsa wood. They assumed that the material has a periodic structure at each length scale (nanoscale, microscale, and mesoscale) and the constituents at each scale are assumed to be perfectly bonded and to remain linear elastic during loading. The elastic properties of the cellulose microfibril, cell wall layers, and the fibers and rays are thus estimated sequentially using nano-, micro- and meso-scale unit cells, respectively (Fig.6(a)). It was demonstrated that a good agreement was found between the model predictions and the available experiment data for most engineering elastic constants reported in the literature, including Young’s moduli and the out-of-plane shear moduli. Model predictions highlight the significance of the ray and fiber cell geometries, cellulose microfibril angle and its crystallinity on the overall elastic properties of wood and more specifically for balsa. This study complements their previous work using multiscale models to investigate the elastic properties of balsa. The second example is about using global load sharing theory to develop accurate analytical predictions for the strength and toughness of hierarchical composites with arbitrary fiber geometries, fiber strengths, interface properties, and number of hierarchical levels^[77]. The model demonstrates that two key material properties at each hierarchical level—A characteristic strength and a characteristic fiber length, control the scalings of composite properties. Through the model, the authors provided simple guidelines for microstructural design of hierarchical composites, including the selection of hierarchical levels, the fiber lengths, the ratio of length scales at successive hierarchical levels, the fiber volume fractions, and the desired properties of the smallest-scale reinforcement.

(2) Topology optimization. The concept of topology optimization was first coined by Bendsoe and Kikuchi in 1988^[78], and since then topology optimization has undergone a tremendous development. Topology optimization gives answers to fundamental engineering questions. For a structure, the ques-

tion is how to place material within a prescribed design domain for optimal structural performance, while for a material the question is how to place constituents within the specified design domain in order to obtain optimal material performance. In recent years, how to integrate topology optimization with additive manufacturing technology to design and fabricate materials/structures with excellent performance and functional characteristics has attracted wide attention^[79-81]. Boddeti et al.^[82] developed a two-scale topology optimization method with the Mori-Tanaka homogenization scheme to simulate the homogenized material response of FRCs where spatial variation of both fiber orientations and fiber volume fraction can be considered, as shown in Fig.6(b). The generated multimaterial microstructures from design can be directly transferred to 3D printing to manufacture and test a series of structures. They later extended the method to continuous fiber-reinforced composites that possess variable stiffness enabled by spatially varying microstructure, which contrasts with traditional fiber-reinforced composites that typically have a fixed, homogenous microstructure and thus constant stiffness^[83]. Recently, Sanders et al.^[84] developed an approach to unify design and manufacturing of spatially varying, hierarchical structures through a multi-microstructure topology optimization formulation with continuous multimicrostructure embedding. The approach can generate an optimized layout of multiple microstructural materials within an optimized macrostructure geometry, manufactured with continuously graded interfaces.

(3) Machine learning (ML). This is a data-driven approach that comes from the field of computer science. ML's goal is to develop general-purpose algorithms that automatically detect patterns in complex data through a training process, and then use those discovered patterns to make predictions about future unknown data. ML is therefore a powerful tool that allows researchers to make generalizations from limited data, rather than exhaustively examining all possibilities. In the context of materials design, basic ML algorithms include linear regression, logistic regression, neural networks, convolu-

tional neural networks, and Gaussian process^[85]. As shown in Fig.6(c), Gu et al.^[86] applied ML to a composite system to accurately and efficiently predict mechanical properties (including strength and toughness) and further generate optimal designs. They first executed an FEM model to solve mechanical properties such as toughness and strength of 2D composites, then they used a general purpose ML framework, TensorFlow, to train the data generated from FEM. Although they have the toughness and strength values from FEM, they only train the ML models with binary information to estimate their ability to reproduce the actual performances based on very limited data. They later extended the method to look for high-performing hierarchical materials where inferior designs are phased out for superior candidates^[87]. Results show that their approach can create microstructural patterns that lead to tougher and stronger materials, which are validated through additive manufacturing and testing. Recently, they used an integrated approach combining FEM, molecular dynamics, and ML to study the effect of constituent materials on the behavior of composites^[88]. It is demonstrated that ML is a much more efficient approach and can generate optimal designs with similar performance to those obtained from an exhaustive search. Apart from composites, ML approach has also been used to accelerate design of cellular materials^[89-91]. For example, Ma et al.^[89] developed a ML-based framework by training a deep neural network with minibatch stochastic gradient descent learning algorithm to predict various mechanical responses due to non-uniform geometric pattern.

(4) Inverse design. At present, the dominated paradigm of material design is primarily in a forward fashion: Given the microstructure, the effective properties are extracted by homogenizing methods. This is inefficient in the sense that one has to determine the desired microstructure topology that meets mechanical property requirements through trial and error. Analytics-based or algorithm-based methods that enable inverse design can considerably accelerate the design process and optimize mechanical properties. If a design problem can be solved using homogenized material models, one can establish an in-

verse design scheme to aid fast and efficient design. For example, Messner^[92] described an inverse homogenization approach for optimizing the mesostructure of lattice-structured materials. The method combines the homogenized material model that calculates the long-wavelength elastic and failure properties of arbitrary lattice materials with a parameterized description of the total design space to generate a parameterized model. The optimally stiff isotruss lattice improves upon the octet truss topology as it has a superior stiffness-to-density ratio while being elastically isotropic (Fig.6(d)). For more complex problems that cannot be analytically addressed, optimization methods such as greedy algorithms and gradient-based algorithms are typically implemented to search for optimal designs without having to explore

the entire design space^[93-94]. However, as pointed by Chen et al.^[85], although optimization methods are computationally efficient, the optimal solution often depends on the initial configuration (the initial value of the design variable) adopted during optimization. As a result, the solutions obtained by these optimization methods will not only vary depending on the initial configuration, but also sometimes fall into local minima or critical points. By contrast, ML algorithms can detect hidden patterns in the data and learn a target function that best maps input variables to an output variable without these shortcomings. Kumar et al.^[95] recently deployed a ML strategy for the inverse design of the spinodal-like metamaterials, which efficiently predicted an optimal topology for a given set of sought properties.

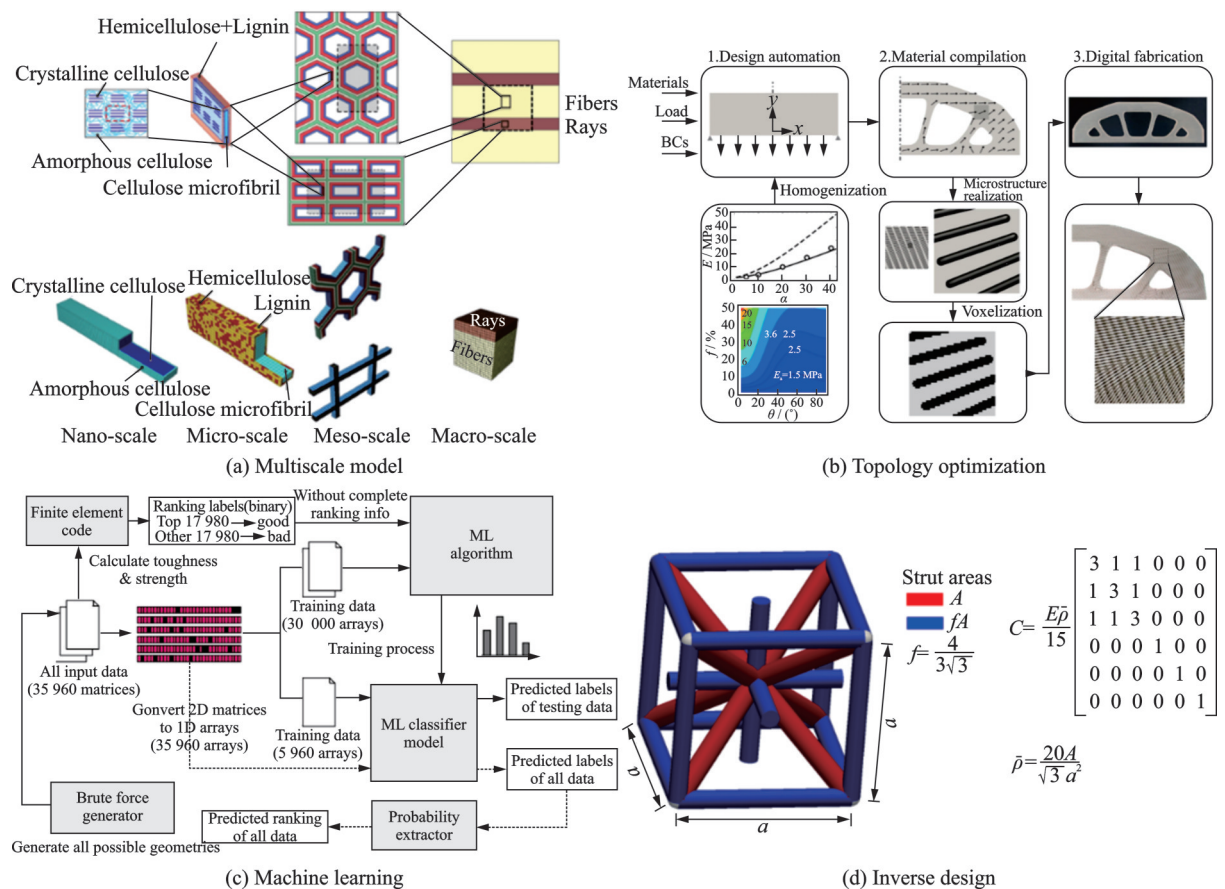


Fig.6 (a) Schematic representation of the hierarchical structure of balsa and discretized material unit cells at different length scales. Adapted with permission from Ref.[18]. © 2017 Elsevier Ltd. (b) Workflow for the simultaneous digital design and manufacture of macroscopic structure topology and material microstructure. Reprinted with permission from Ref. [82]. Copyright © 2018, The Authors. (c) The flow chart shows the ML approach using the linear model for an 8 by 8 system. Reprinted with permission from Ref.[86]. © 2017 Elsevier Ltd. (d) The isotruss unit cell topology that shows the simple cubic cell, rather than the primitive BCC cell described by the optimized parameters. Reprinted with permission from Ref.[92]. © 2016 Elsevier Ltd

2 3D Printing Manufacturing Process Modeling

The final performance of McMI3DPMs is largely influenced by 3D printing manufacturing process. As mentioned in the introduction section, the process of material forming involves a variety of complex physical phenomena and layer-by-layer addition characteristics, which lead to large processing history differences at different areas. When processing history differences are further coupled with component behavior, it becomes difficult to predict the evolution of stress and interlayer strength during printing, resulting in an inaccurate description of defects (such as residual stresses, geometric distortions, and microvoids) and thus the overall performance of the printed material. In the past few decades, both experimental and theoretical studies have been carried out to understand the mechanics of 3D printing processing process. In this section, we will review the major advances in 3D printing manufacturing process modeling from three aspects: Resin photocuring-based 3D printing, powder sintering-based 3D printing, as well as material extrusion-based 3D printing. Our focus is on polymer 3D printing manufacturing process, and this is based on two considerations: First, polymers are lightweight compared with metals and ceramics. Advanced McMI3DPMs should contain polymer components as future candidates for next-generation structural materials; Second, polymer 3D printing technologies are relatively mature compared with non-polymer ones, and polymer architectures created by ink- and light-based 3D printing approaches can be transformed into metallic and ceramic structures that are difficult to directly print at various length scales.

2.1 Resin photocuring-based 3D printing

Resin photocuring-based 3D printing techniques mainly contain stereolithography (SLA), digital light processing (DLP), continuous liquid interface production (CLIP)^[96], and two-photon polymerization (2PP). Unlike SLA which uses point-source illumination to cure one volume element at a time, DLP and CLIP rely on digital mask-mediated

images to selectively pattern liquid resin in a layer-by-layer fashion (Fig.7(a)), thus enabling remarkably fast and high-resolution printing. The commonly used raw materials in resin photocuring-based 3D printing are photopolymerizable resins (Fig.7(b)), which yield either rigid or soft thermoset polymers after printing. Therefore, resin photocuring-based 3D printing are mostly used to produce functional parts. However, because of their capabilities in high-resolution printing, researchers have recently attempted to use this type of printing technology to manufacture metals and ceramics in ordered structures, i. e., by post-processing produced polymer parts through coating a layer of metals/ceramics^[27-28, 97] or by pretreating the resin through mixing resin with fine metal/ceramic powders^[98-100]. Plus, new photosensitive polymeric materials with excellent mechanical properties have been developed rapidly in recent years and have been used to verify the mechanism of new structural design^[101-103]. The resin photocuring-based 3D printing technologies are gradually expanding into structural applications.

In resin photocuring-based 3D printing, the fundamental material solidification mechanism is photopolymerization^[104-107], which primarily involves four reaction kinetics mechanisms: Initiation, propagation, termination, and inhibition. As illustrated in Fig.7(c), the initiation reaction starts with absorption of light to decompose one initiator into two radicals. Then the radical reacts with monomer to form a growing polymer chain of which the rate is determined by k_i . The other type of chain initiation is reinitiation of inhibited chains, viz., an inhibited chain reacts with monomer to reform an actively growing chain. The propagation reaction can be represented by a single reaction where the kinetic constant for propagation is k_p . Chain termination occurs through two different mechanisms: The first is bimolecular termination which can be lumped into a single reaction having kinetic constant k_t ; the second is primary radical termination, where a primary radical reacts with a growing polymer chain to form dead polymer. The kinetic constant for this process is k_{tp} , differing from the bimolecular k_t . The final reaction is chain inhibition, in which inhibitor species, such

as molecular oxygen or deliberately added inhibitors, react with a growing chain to form a relatively unreactive species, and the kinetic constant for this process is k_z . When the photopolymerization process comes to a 3D printing scenario, there is a trade-off between process speed and forming precision roots on the diffusion-limited kinetics of photopolymerization. Fang et al.^[108] used a numerical model to investigate the influence of diffusion dominant effect under high photon flux and proposed a solution of pulsed laser curing in order to realize sub-micron resolution in high speed SLA process. They later developed a process model and obtained all key parameters from experimental measurements to study the photon-induced curing behavior of the resin in DLP^[19]. By justifying the role of UV doping, the curing depth can be effectively reduced without affecting the chemical property of the resin, thus enabling a range of complex 3D microstructures with a minimum characteristic of 0.6 μm .

Volume shrinkage, which originates from the macroscopic volume reduction caused by molecular crosslinking in the process of photopolymerization, is one of the most common adverse phenomena in resin photocuring-based techniques. Large volume shrinkage can cause severe residual stress and warpage, significantly reducing printing accuracy and material properties. Dewaele et al.^[109] experimentally found an univocal relationship between the volume contraction and the actual number of vinyl double bonds converted into single ones. The relationship can help in finding solutions to the polymerization shrinkage problem. For example, by adding molecules to allow a decrease in the number of double bonds converted per unit volume of resin matrix, a reduction of the polymerization shrinkage due to the chemical reaction may be expected. Lu et al.^[110] suggested to cure samples at a low temperature so that the resulted volume shrinkage was less than that at room temperature, while at the same time the mechanical properties remained similar. A model of polymerization kinetics based on free volume theory was introduced to predict and analyze the curing shrinkage and kinetic parameters of an acrylate-based ultraviolet-embossing resist^[111], and the ex-

perimental results were in good agreement with the simulated results of the conversion behavior.

Due to the complex photopolymerization mechanism, together with the volume shrinkage effects, it is difficult to accurately describe the deformation behavior of materials during curing. Some early work generally ignored the detailed curing kinetics and focused on curing reaction-induced shrinkage strain, thermal expansion, temperature change, as well as finite strain thermoviscoelasticity. Representative studies in this aspect are carried out by Lion et al.^[112], Hossain et al.^[113-116], and others^[117-118]. Among them, Mergheim et al.^[118-119] also considered the curing-induced damage when studying the mechanical behavior of thermosetting adhesives. Recently, Wu et al.^[120] proposed a new model that fully takes into account the reaction kinetics and the coupling between deformation and property evolution during free radical photopolymerization. In their model, the coupling between deformation and performance evolution is addressed by introducing the concept of "phase evolution", as shown in Fig.7(d).

In multilayer printing, the physics discussed above will couple with the layer-by-layer addition process, resulting in residual stress and shape distortions in the printed part. Due to the previous research on the photocuring physics and the bright application prospect of resin photocuring-based 3D printing techniques, this problem has increasingly gained attention and been studied. The mostly used research means is finite element analysis, which can conveniently consider the degree of conversion-dependent shrinkage, the material behavior, as well as the layer-by-layer addition process. Early simulation efforts have concentrated in the SLA printing process, such as the work conducted by Bugada et al.^[121], Xu et al.^[122], and Huang et al.^[123], while the recent focus is moving toward the DLP and CLIP process. For example, Wang et al.^[124] developed a coarse-grained molecular dynamics simulation approach to model the printing process of CLIP. Simulations show that the quality of the shape of the 3D printed objects is determined by a fine interplay between elastic, capillary, and friction forces. Wu et al.^[125] established an analytical model that com-

bined photopolymerization reaction kinetics and Euler-Bernoulli beam theory to study UV post-curing induced shape distortion of thin structures prepared by DLP 3D printing. Very recently, Zhang et al.^[126] and Westbeek et al.^[127] proposed their own finite element-based approaches to study the geometrical defects of DLP-printed parts due to

shrinkage effects. Since their models have considered various physics involved in the printing process, the simulation results can well reproduce the experimentally measured shape distortions (Fig.7(e)), thus providing an approach for the design and optimization of photocurable 3D printing components.

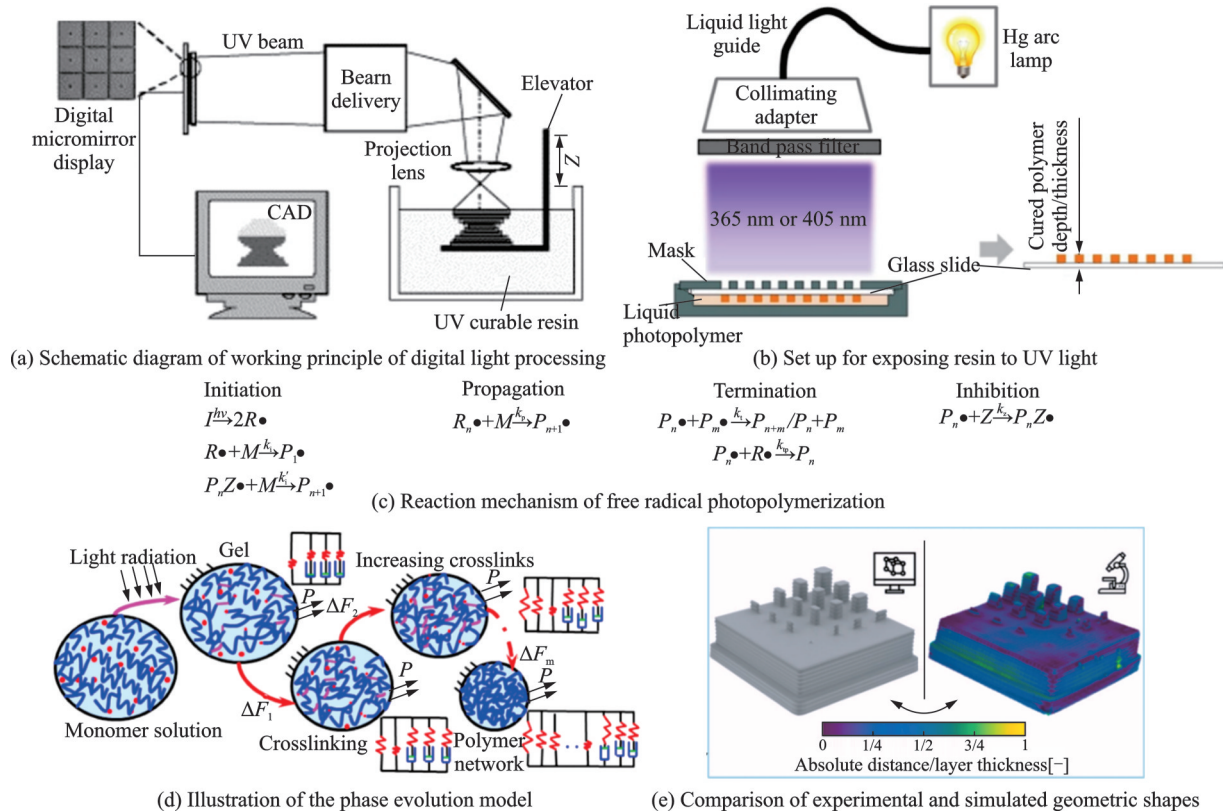


Fig.7 (a) Schematic diagram of working principle of digital light processing. Reprinted with permission from Ref.[19]. Copyright © 2005 Elsevier B.V. (b) Set up for exposing resin to UV light. Reprinted with permission from Ref.[128]. Published by Elsevier B.V. (c) Reaction mechanism of free radical photopolymerization. (d) Diagram of illustrating the phase evolution model. Reprinted with permission from Ref.[120]. © 2017 Elsevier Ltd. (e) Comparison of experimental and simulated geometric shapes. Adapted with permission from Ref.[127]. © 2021 The Authors. Published by Elsevier B.V

2.2 Powder sintering-based 3D printing

Printing techniques belonging to powder sintering-based 3D printing mainly include laser selective sintering (SLS) and multi-jet fusion (MJF). The raw material used in this type of 3D printing is in the form of powders and the obtained material are mainly semi-crystalline thermoplastic polymers^[129-131]. In addition to the most commonly used nylon (PA12)^[132], high-performance engineering plastics such as polyether ether ketone (PEEK) and polyphenylene sulfide (PPS), and low-cost general plastics such as polypropylene (PP) and polyethylene (PE) have al-

so attracted researchers' attention in recent years.

The powder sintering-based 3D printing starts with a beam of laser (in SLS) or infrared light (in MJF) to irradiate powder particles to allow them to absorb heat to change physical states (Fig.8(a)), and when the environment temperature in the irradiated spot is raised up to the range of the melting temperature (Fig.8(b)), particles will be able to flow and fuse or sinter together driven by surface tension^[133-134]. At the particle scale, fusion involves neck formation between adjacent particles and changes in particle shape to minimize the total energy (thermal and mechanical) of the system (Fig.8(c)).

With the development of the fusion process, the pores between the particles gradually decrease, and the initially loosely packed particles become bulk porous materials where the porosity strongly depends on the degree of fusion. The temperature history, as well as the thermomechanical behavior of the particles, primarily govern the fusion process of particles. Balemans et al.^[135] developed a finite element-based computational model to study the material and process parameters concerning the melt flow of the PA12 powder particles. By considering temperature-dependent viscosity, process parameters, and convective heat transfer, they concluded that an optimal sintering process had a low ambient temperature that was a narrow beam width with enough power to heat the particles and only a few degrees above the melting temperature.

As the layer-by-layer printing progresses, new areas are fused and added to the already fused main structure, enabling additive production of the final 3D parts. The printing quality and the mechanical behavior of the produced part depend on many printing conditions, including irradiation energy density, powder bed temperature, layer thickness, and particle size, etc. If these conditions are not well controlled, the fusion cannot be carried out very thoroughly and the resulting material may appear voids (Fig.8(d)), leading to degradation of material properties^[20, 136]. Mokrane et al.^[137] investigated porosity distribution and densification of the SLS-printed part through a numerical tool based on the finite volume method. Their analytical tool takes into account thermo-physical transient phenomena in the SLS process, allowing the influence of process parameters to be investigated. Chen et al.^[138] found that the void defects had a great influence on the deformation of PA12 printed by MJF, and they developed a finite-strain viscoelastic-viscoplastic model aiming at capturing the behavior of the material. In their model, they phenomenologically introduced a scalar variable to characterize the material damage induced by accumulated plastic deformation. Through implementing the model into finite element simulation, they revealed that the low tensile ductility of MJF PA12 was caused by the increase in strain localization and narrowing of the shear band.

Apart from the porosity problem, the thermal stress caused by temperature cycles experienced by powders during printing can result in shape distortion, reducing the geometric accuracy of the material's structure at different length scales (Fig.8(e)). Childs et al.^[139] analyzed the thermal and powder densification of SLS process for amorphous polycarbonate. Their analysis showed that the changes in the activation energy and heat capacity of the polymer were the main factors that affect the densification and linear accuracy due to sintering. Dai and Shaw^[140] later proposed a finite element analysis to investigate the effect of laser scanning patterns on residual thermal stresses and distortion. They found that a proper selection of the laser scanning pattern can be used to minimize the out-of-plane distortion of a layer, and distortion is mainly caused by transient thermal stresses rather than residual thermal stresses. Raghunath et al.^[141] used Taguchi method to study the effect of parameters, namely laser power, beam speed, hatch spacing, part bed temperature and scan length on shrinkage for better accuracy. Dong et al.^[142] developed a transient three-dimensional finite element model to simulate the phase transition during SLS, which took into account the thermal and sintering phenomena involved in the process. The predicted results show a linear dependence between the laser power and the maximum temperature on the powder bed surface. High heat diffusion in the powder bed is obtained by higher laser power, lower laser speed, higher preheating temperature and lower laser beam diameter. Peyre et al.^[143] carried out both experiments and numerical simulations to estimate thermal cycles and resulting fusion depths obtained during SLS of PA12 and PEKK, and the influence of process parameters on the thermal cycles experienced by surface layers were well addressed. In 2018, Mokrane et al.^[137] focused on the global view of simulating an SLS process of polymer powder and developed a multiphysical model that incorporated thermo-physical properties, laser power distribution, fusion, coalescence, gas diffusion, and crystallization. The numerical tool was validated by experiments. Recently, Shen et al.^[144] developed a comprehensive thermomechanical model to predict the temperature, degree of crystallization, residual stress, and strain in the

SLS process for polymeric powders. The model is used together with a finite element method to simu-

late the thermal and mechanical behavior of PA12 during the heating and cooling processes.

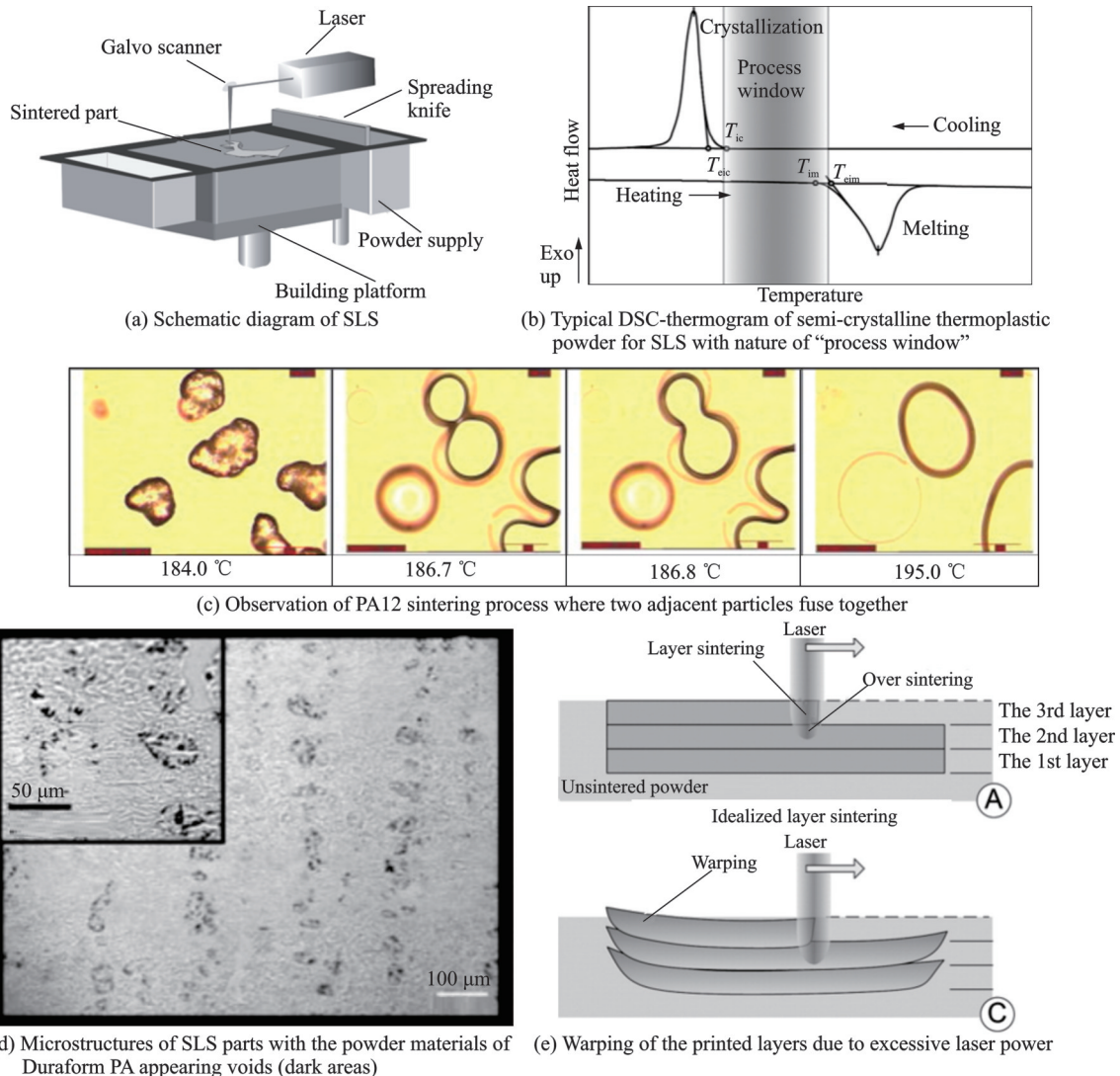


Fig.8 (a) Schematic diagram of SLS. Reprinted with permission from Ref.[20]. Copyright © 2007 Published by Elsevier Ltd. (b) Typical DSC-thermogram of semi-crystalline thermoplastic powder for SLS with nature of "process window". Adapted with permission from Ref.[145]. © 2017 Elsevier Ltd. (c) Observation of PA12 sintering process where two adjacent particles fuse together. Reprinted with permission from Ref.[146]. Copyright © 2014 Elsevier B.V. (d) Microstructures of SLS parts with the powder materials of Duraform PA appearing voids (dark areas). Adapted with permission from Ref.[147]. Copyright © 2012 Elsevier Ltd. (e) Warping of the printed layers due to excessive laser power. Adapted with permission from Ref.[148]. Copyright © 2009 Wiley Periodicals, Inc

2.3 Material extrusion-based 3D printing

Fused deposition modeling (FDM) and fiber-reinforced direct-ink writing (FRC-DIW) are two main printing techniques that rely on material extrusion to fabricate 3D parts. For FRC-DIW, the extruded filament contains a matrix phase, which is in a highly viscous, not cured state, and a short fiber phase. During the extrusion process, the viscous

shear-thinning matrix phase is extruded from the nozzle to the previous layer and merges with the previous layer, while the short fibers mixed in the filament come out from the nozzle together with the matrix. Since the fibers are subjected to shearing forces during the extrusion process, they align along the print path after exiting the nozzle, resulting in unidirectional enhancement effects. The green part is usu-

ally cured by two methods: One is in situ curing of the extruded filament using UV light during the printing process, and the other is to transfer the entire part to a thermal environment for thermal curing after the print is finished. The polymer matrix used in FRC-DIW are mostly thermosets, and the reinforcement can be glass or carbon fibers. Modeling of FRC-DIW, or even just DIW (without fiber reinforcement) printing process is scarce, with only a few studies reported on material flow behavior during extrusion^[149]. Therefore, our next focus is on FDM, although FRC-DIW has grown rapidly in recent years and holds great promise in manufacturing multi-component ordered structures^[150].

The material forming mechanism in FDM is different from that in FRC-DIW. In FDM, although the raw material is also in the form of polymer filaments, the used polymer filaments are usually non-crystalline (amorphous) thermoplastic polymer materials. Through proper process control and composition modification, semi-crystalline polymer filaments (such as PA6, PEEK, etc.) have been increasingly developed and applied in recent years. During the extrusion process (Fig.9(a)), the nozzle works at a temperature higher than the glass transition temperature of the material to allow the semi-molten filament to be easily extruded out. Once out of the nozzle and deposited on top of the previous layer, the extruded filament segment will come into contact with the surrounding filaments (Fig.9(b)), which will remelt to fuse with the deposited filament segment. The fusion or bonding processing encompasses multiple physics in the binding region, including temperature increase^[151], diffusion^[152-153] (Fig.9(c)), and cooling. Lou et al.^[154] recently proposed a transient updated Lagrangian finite element formulation for bond formation in fused deposition modeling process, where the effects of initial configuration and boundary conditions and gravity on the bond formation in the FDM process were studied.

Due to the layer-by-layer addition, rapid cooling, and phase change characteristics, there is a large thermal gradient in the FDM-printed parts, which leads to the generation of residual stress. When the print is finished and the printed part is re-

moved from the building plate, the residual stress must be released, which can introduce curling, warping, and delamination problems. A mathematical model that incorporated various processing factors including the deposition layer number, the stacking section length, the chamber temperature, and the material linear shrinkage rate was proposed by Wang et al. to study the warp deformation of FDM-printed parts^[155]. The model can provide a scientific tool for controlling and adjusting the undesired deformation. Zhang et al.^[156] developed a finite element analysis model using element activations to simulate the mechanical and thermal phenomena in FDM and further residual stress distribution and part distortion. They then used the numerical model to study the effects of the scan speed, the layer thickness, and the road width on part distortions^[157] (Fig.9(d)). Liu et al.^[158] proposed a theoretical model based on the theory of elastic thin plates in thermoelasticity in order to reveal the distortion mechanism of PLA thin-plate part in the FDM process. Their theoretical results were well validated by experimental measurements via a 3D laser scanner. Recently, Armillotta et al.^[159] found that the maximum distortion occurred at intermediate values of part height through experiments and statistical analysis, which was not observed in previous studies. They further developed analytic equations to explain the new effect of distortions: One is based on the extension of thermal stresses to multiple layers due to heat conduction from the last deposited layer, and the other is based on the hypotheses of the occurrence of bending stresses beyond the yield point of the material. Crystallization can also be taken into account when studying warpage, as done by Fitzharris et al.^[160], who adapted the previous process simulation models to investigate warpage of FDM parts made with a high-performance semicrystalline polymer. The simulation models suggested that the coefficient of thermal expansion (CTE) has the largest impact on the FDM part warpage, and decreasing CTE resulted in a decrease in warpage by the same factor.

One of the most prominent features of the mechanical behavior of FDM-printed materials should

be anisotropy^[161]. An early study was carried out to understand the effect that FDM build parameters had on the anisotropic material properties^[161]. The process parameters of FDM include raster orientation, air gap, bead width, color, and model temperature. Tensile strengths and compressive strengths of directionally fabricated ABS specimens were measured and compared with injection molded counterparts. By experimentally characterizing the influence of printing parameters on the mechanical response of ABS specimens printed by FDM, Garzon-Hernandez et al.^[162] recently proposed a continuum model to describe the macroscale behavior of FDM thermoplastics. The model is formulated for finite deformations within a thermodynamically consistent

framework where anisotropic hyperelasticity related to a transversely isotropic distribution of porous and macroscopic stiffness dependent on printing processing are taken into account (Fig.9(e)). The anisotropy will also affect the strength of FDM-printed parts. Mirzendehtel et al.^[163] established the anisotropic strength criterion of additive manufacturing materials by using Tsai-Wu failure criterion, and the experimental strength of the designed topological structure was significantly superior to the results of traditional stress-constrained topology optimization. Unlike previous methods that usually require experimental strength data as a prediction input, the approach developed by Bartolai et al.^[164] to predict the strength of polymer parts produced by FDM is

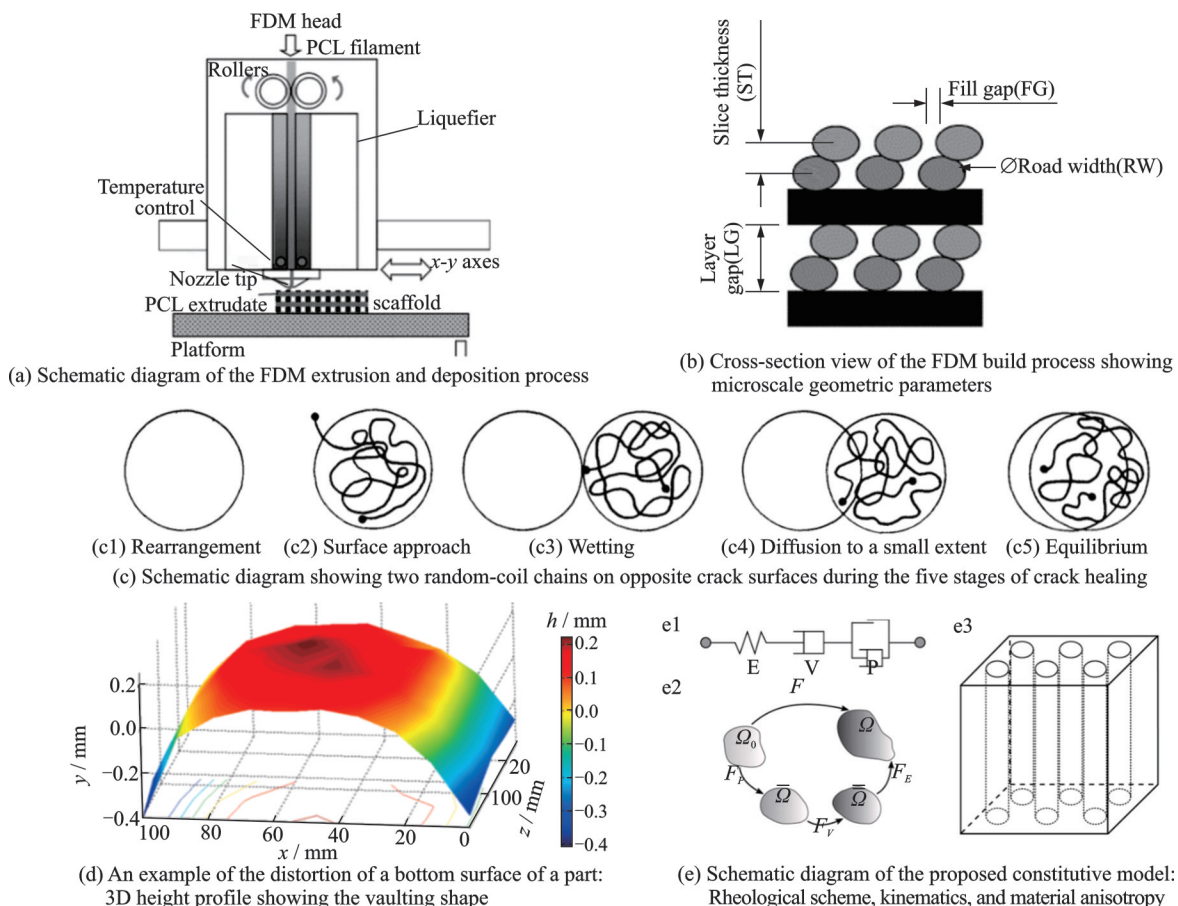


Fig.9 (a) Schematic diagram of the FDM extrusion and deposition process. Reprinted with permission from Ref.[21]. Copyright © 2001 Elsevier Science Ltd. (b) Cross-section view of the FDM build process showing microscale geometric parameters. Adapted with permission from Ref.[21]. Copyright © 2001 Elsevier Science Ltd. (c) Schematic diagram showing two random-coil chains on opposite crack surfaces during the five stages of crack healing. Adapted with permission from Ref.[152]. Rights managed by AIP Publishing. (d) An example of the distortion of a bottom surface of a part: 3D height profile showing the vaulting shape. Reprinted with permission from Ref.[157]. Copyright © 2008, © SAGE Publications. (e) Schematic diagram of the proposed constitutive model: (e1) Rheological scheme, (e2) kinematics, and (e3) material anisotropy. Adapted with permission from Ref.[162]. © 2020 The Authors, Published by Elsevier Ltd

based on the strength of interfaces using polymer welding theory, polymer rheology, and temperature history of the interface. Thus, once the basic parameters related to material composition are determined, the method is independent of material and build orientation.

3 Defect Characterization and Property Evaluation

Limited by the specific printing process and the quality of raw materials, there are inevitably defects in printed matter where the location, shape, size and distribution information is unknown. These defects have significant influence on the performance and reliability of as-printed matter. Therefore, defect characterization and property evaluation are critical for McMI3DPMs to move from conceptual design to practical application. In this section, we mainly review the recent progress in this regard from defect detection and mechanical properties characterization across scales.

3.1 Defect detection: During and after manufacturing process

Defect inspection methods are important for reducing manufactured defects and improving the surface quality and mechanical properties of 3D-printed components. At present, these methods can be divided into in situ and ex situ methods.

Holzmond et al.^[22] presented the use of a 3D digital image correlation (3D-DIC) system as a non-destructive in situ measurement technique to monitor the surface geometry of a FDM-printed part. As shown in Fig.10(a) (left), the detected defects include both local area defects, such as a blob of filament, and global defects, such as low flow. Although various surface defects can be detected, the system requires pauses or stops during the printing process to conduct print adjustments and is not capable of real-time correcting printing conditions. Jin et al.^[165] developed a real-time monitoring and autonomous correction system for FDM manufacturing process, where a deep learning model and a feedback loop are used to modify printing parameters iteratively and adaptively. Their machine learning

based 3D-printing system consists of two parts: A post-training procedure and an in-situ real-time monitoring and refining section (Fig.10(a), right). In the first step, a CNN classification model is trained using a ResNet 50 architecture. After the completion of the training period, during the 3D-printing process, real-time images are continuously fed into the model and classified to obtain the current printing condition. The same researchers have also developed a method based on computer vision and strain measurements to detect and predict interlayer imperfections such as delamination and warping in the FDM-printed parts^[166]. Deep learning algorithms were used to classify and detect delamination conditions based on camera images, and a novel setup based on strain gauge measurements was established to measure and predict the tendency of warping.

Optical monitoring has the advantage of observing surface defects in a non-destructive manner. However, when used to detect internal defects, samples must be cut open for sectional characterization. Recently, X-ray computed tomography (XCT), a method for generating 3D imaged volumes from 2D X-ray image slices, has become a powerful tool in capturing the morphology and distribution of process-induced defects of additive manufactured architected materials, in particular the internal defects^[167]. For example, based on 3D micro-XCT scanning, Cao et al.^[168] and Geng et al.^[169] have analyzed the geometrical errors and fabrication defects of 3D lattices, including strut porosity, strut thickness variation and strut waviness (Fig.10(b), left). By constructing the obtained tomographic images through algorithms, the detailed information of the shape, position and distribution of defects can be visualized in 3D space, thus proving significant convenience for subsequent analysis. In addition, synchrotron micro-XCT 3D imaging was also employed for quantifying the effect of defects on the compression mechanical performances of TPMS cylinder shell structures fabricated with projection micro-stereolithography 3D printing technique (Fig.10(b), right). It is found that the thickness of the shell along the vertical direction was larger than

that of the shell along the horizontal direction^[170]. Although exhibiting a set of advantages, XCT systems are relatively expensive and can hardly achieve full-field characterization of deep interior due to the

limitation of penetrating ability. In addition, XCT is usually used for post-production analysis and thus may not have the potential advantages of in situ processing such as real-time correction of printing parameters.

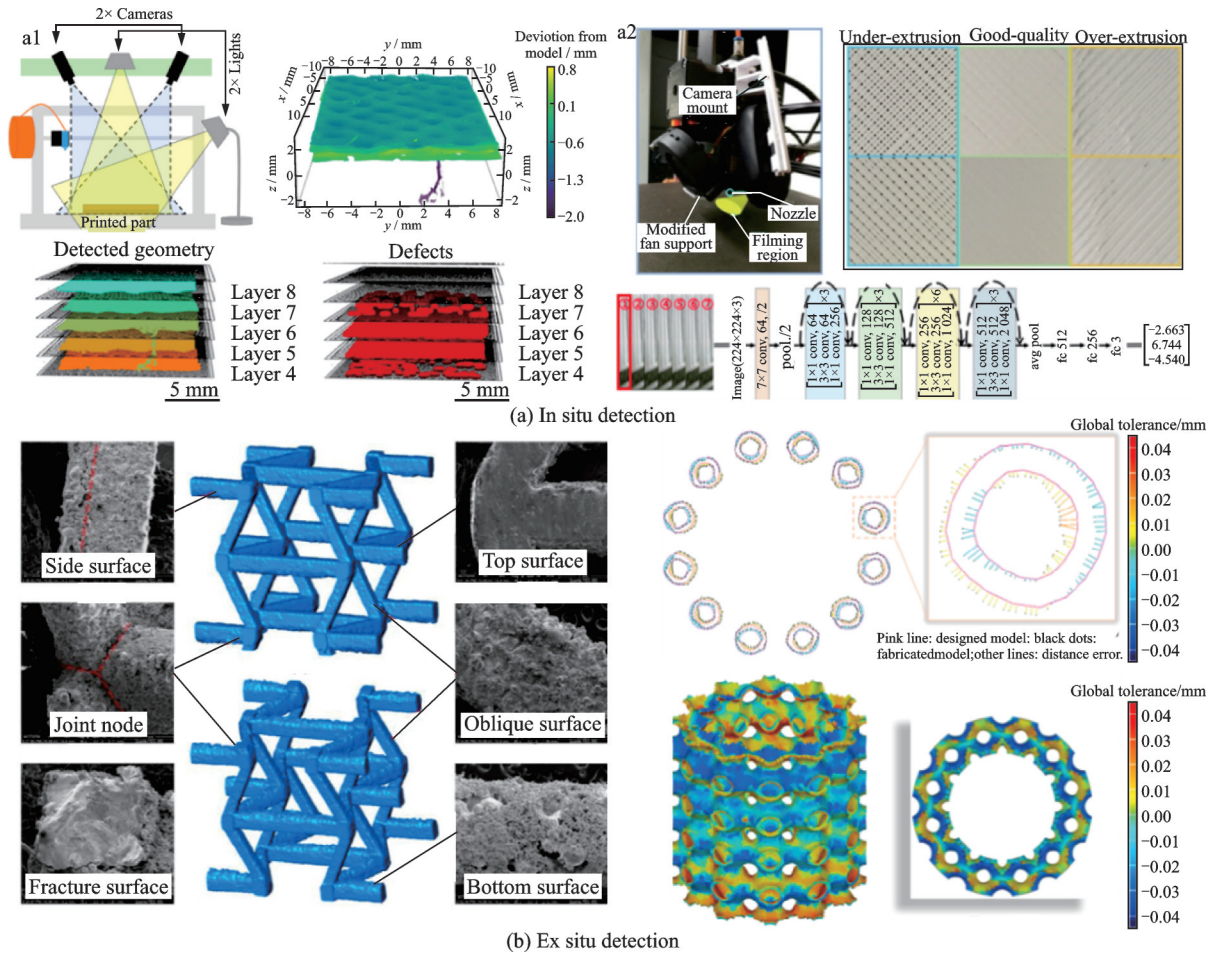


Fig.10 (a) In situ detection: (a1) Defect detection of a low or high z height relative to the previous layer, indicative of flow problems (Adapted with permission from Ref.[22]. © 2017 Elsevier B. V.), and (a2) six 3D-printed blocks under different printing qualities categories of under-extrusion, good-quality, and over-extrusion, and the used modified CNN model in the system based on ResNet 50 architecture (Adapted with permission from Ref.[165]. © 2019 Society of Manufacturing Engineers). (b) Ex situ detection: (b1) Details of the reconstructed unit cell and the printed unit cell morphology (Reprinted with permission from Ref.[169]. © 2019 Elsevier Ltd.), and (b2) comparison of the geometry between the as-fabricated and designed model (Reprinted with permission from Ref.[170]. © 2021 Elsevier Ltd.)

3.2 Mechanical properties characterization across scales

McMI3DPMs involve structures at multiple length scales, and these underlying (nanoscale, microscale, and mesoscale) structures determine the materials' macroscale mechanical properties. New mechanical measurement principles, theories, and methods are needed to characterize McMI3DPMs across scales.

In order to accurately characterize the mechanical behavior of additive manufactured microlattices, high resolution in situ loading and observation techniques are required to capture the deformation events of microlattices occurring at very small scales. One method is to couple scanning electron microscope (SEM) with nanoindentation devices. For example, in order to characterize high-strength cellular ceramic composites, Bauer et al.^[23] per-

formed loading-rate-controlled uniaxial in situ and ex situ compression tests by nanoindentation with a diamond flat punch tip $100\ \mu\text{m}$ in diameter (Fig.11(a)). Load-displacement curves were recorded and extracted to obtain engineering stress-strain curves, which were further used to compute Young's modulus and compressive strength.

Although SEM-based in situ loading can effectively obtain surface mechanical quantities, internal damage of materials cannot be accessed by surface observation. However, the initiation and evolution of internal damage often determine how the material fails. It has been demonstrated that synchrotron XCT-based in situ loading techniques have the ability to extract the internal information of samples during loading^[171-172]. Bale et al.^[173] used synchrotron XCT to resolve sequences of microcrack damage of ceramic matrix composites with cracks grow under loads up to $1\ 750\ ^\circ\text{C}$ (Fig.11(b)). The results contain vital information pertaining to the underlying failure mechanisms within ceramic composites that

can be used to optimize their performance. By combining the image information obtained from in situ XCT-based loading with numerical analysis, image-based numerical computing techniques can be developed to predict mechanical properties of materials. For example, Geng et al.^[169] developed an image-based finite element method to predict the deformation behavior of re-entrant lattice structures. Since the reconstructed geometric model contains real geometric information (e.g., defects), the prediction results can better reflect the real situation, including elastic modulus, strength and failure mechanism. Currently, XCT-based in situ loading techniques have been routinely used to investigate deformation and failure behavior of various 3D-printed advanced materials^[174].

Due to the discrete features at the microscale, traditional testing philosophy may sometimes not be applicable to characterize the macroscale properties of metamaterials. Shaikeea et al.^[175] have recently shown that for metamaterial specimens consisting of

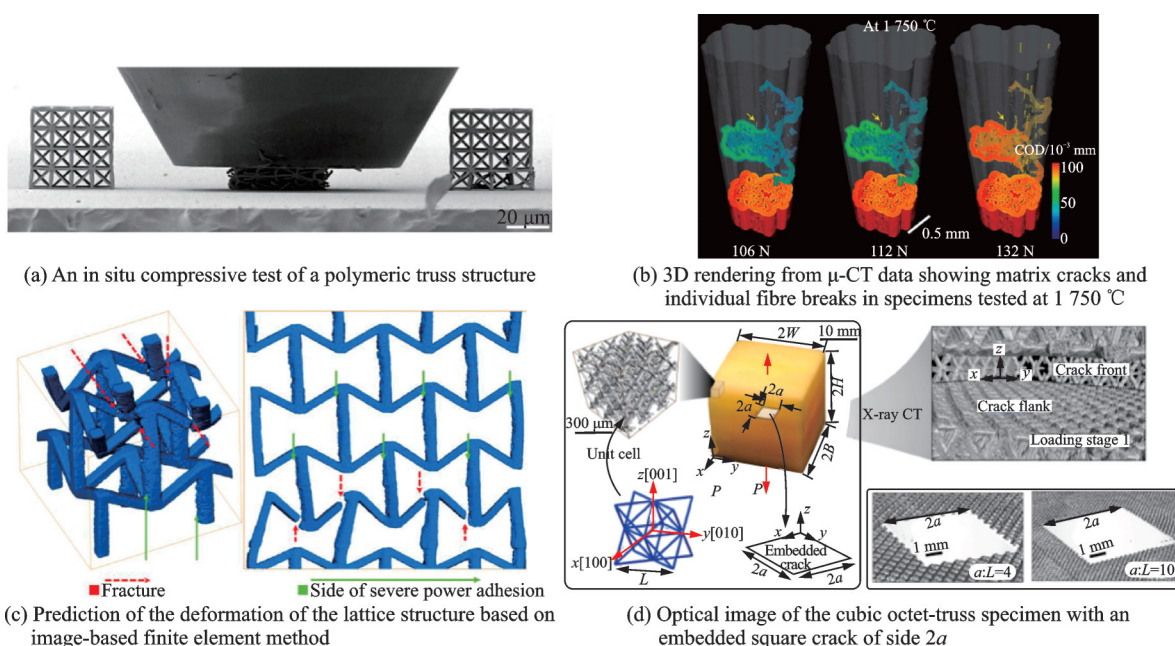


Fig.11 (a) An in situ compressive test of a polymeric truss structure. Adapted with permission from Ref.[23]. (b) 3D rendering from μ -CT data showing matrix cracks and individual fibre breaks in specimens tested at $1\ 750\ ^\circ\text{C}$. The red-blue colour scheme indicates opening displacements of matrix cracks, quantified by the processing of 3D tomography data. Yellow arrows indicate cylindrical holes remaining after relaxation of broken fibres. Adapted with permission from Ref.[173]. Copyright © 2012, Springer Nature Limited. (c) Prediction of the deformation of the lattice structure based on image-based finite element method. Reprinted with permission from Ref.[169]. © 2019 Elsevier Ltd. (d) Optical image of the cubic octet-truss specimen with an embedded square crack of side $2a$. Adapted with permission from Ref.[175]. Copyright © 2022, The Authors, under exclusive licence to Springer Nature Limited

millions of unit cells, not only is the stress intensity factor used in conventional elastic fracture mechanics insufficient for characterizing fracture, but that traditional fracture testing schemes are also inappropriate. As they stated, the discreteness of the octet-truss metamaterial implies that a mathematically sharp crack is not present, and hence a strut that undergoes either tensile fracture or elastic buckling failure is at finite distance from the ill-defined crack front; in such a scenario, the non-singular T-stress terms become similar to the K_I terms and affect elastic fracture of the octet-truss, creating the need for an enrichment of conventional elastic fracture mechanics to describe fracture of elastic metamaterials irrespective of their microstructure.

4 Conclusions and Outlook

Through borrowing ingenious design principles from nature and exploiting advanced 3D printing techniques, many McMI3DPMs have been developed and are expected to gain important applications in many fields. This review summarizes the major progress in McMI3DPMs in recent years from three aspects: Structural design, manufacturing processing modeling, and defect characterization and property evaluation. The main thread of the review (structure-process-property) actually reflects the prominent feature of the materials like McMI3DPMs: Superior performance is highly dependent on structural complexity and the manufacturing process capable of bringing about this complexity.

Although many advances have been achieved, the present research in McMI3DPMs is still in the stage of conceptual designs and the stage of exploration of printing process for improving material properties. The underlying scientific questions related to McMI3DPMs have not been thoroughly studied and well resolved. Part of the reason for this, understandably, is the immaturity of 3D printing technology, particularly in terms of how to print materials across wider levels of composition and structure, and how to achieve scalability. In the future, more efforts should be made to further advance the development of this emerging field. Key research direc-

tions and noteworthy scientific questions include:

(1) New design principles that enable higher strength and toughness. In the engineering field, the approach to pursue high strength and high toughness structural materials is often inefficient, i.e., at the cost of high energy (including high weight, and high synthesis temperature and pressure). Nature, by contrast, has the ability to reduce complexity to simplicity. This can be well illustrated by biomineralized structural materials, which can synthesize themselves with complex structural characteristics and excellent properties by using only seawater and simple organic components. The superb design skills hidden behind various biological materials are worthy of human exploration and learning. Recently, some researchers have turned their attention to deep-sea animals that living in extremely high hydrostatic pressure environments^[176-177], a promising direction to explore more fundamental principles that contribute to robust mechanical properties (e.g., high compressive strength and damage tolerance).

(2) Reduced-order multiscale modeling and topology optimization. Multiscale modeling is an essential tool for analyzing the mechanical behavior of McMI3DPMs, and it is also the cornerstone for developing efficient topology optimization methods to optimize the topology of McMI3DPMs. However, due to the increasing complexity of 3D architectures, ordinary multiscale models are unable to provide accurate structure-property relations with less computational costs. It is very promising to develop reduced-order models that reduce computational time and data storage requirements. In recent years, the combination of data clustering algorithms and efficient analysis of heterogeneous material problem of unit cell method has given rise to a class of data-driven reduced-order models^[178] that can efficiently and accurately predict the nonlinear equivalent properties while reducing computational cost, including the self-consistent clustering based on discrete Lippmann-Schwinger equation analysis, Hashin-Shtrikman (H-S) type finite element method based on H-S variational principle, and cluster analysis method based on finite element method.

(3) Integrated modeling of additive manufac-

turing and material mechanical behavior. At present, the research on 3D printing material forming process modeling and 3D printing material mechanical behavior analysis is basically in a separate state. Intensive experimental measurements of printed materials are required to feed the phenomenological theoretical model before it can be used to predict material behavior. This is time-consuming and laborious, and the properties of the material of interest cannot be assessed before printing. Integrated modeling of 3D printing manufacturing process and material mechanical behavior, without experiment involvement, is thus promising. To this end, it is necessary to conduct high-fidelity multi-physical field simulation of the manufacturing process for transferring as much detail (heterogeneity, anisotropy, defects, etc.) as possible to the subsequent description of mechanical behavior. This will undoubtedly involve a large amount of computational costs. New computational models need to be developed to balance computational efficiency and precision.

(4) In situ defect detection and correlations between defects and material failure mechanisms. The ultimate goal is to enable the model to not only capture forward the effect of processing parameters on final performance, but also to make its own judgments and decisions during the manufacturing process to adjust the final material. In order to achieve this goal, we have to look for capabilities to perform field diagnostics and real-time data processing during the manufacturing and loading stages. Meanwhile, studies that relate the acquired data to material failure behavior should be conducted to identify failure mechanisms and establish reliable strength models. Tools from data science, such as machine learning, might be used in conjunction with physical laws to deal with large amounts of processing data and complex correlations between defects and material failure mechanisms.

References

- [1] TRUBY R L, LEWIS J A. Printing soft matter in three dimensions[J]. *Nature*, 2016, 540(7633): 371-378.
- [2] RAFIEE M, FARAHANI R D, THERRIAULT D. Multi-material 3D and 4D printing: A survey[J]. *Advanced Science*, 2020, 7(12): 1902307.
- [3] UZEL S G M, WEEKS R D, ERIKSSON M, et al. Multimaterial multinozzle adaptive 3D printing of soft materials[J]. *Advanced Materials Technologies*, 2022, 7(8): 2101710.
- [4] ZHANG Hang, WU Jun, ZHANG Yihui, et al. Multistable mechanical metamaterials: A brief review[J]. *Transactions of Nanjing University of Aeronautics & Astronautics*, 2021, 38(1): 1-17.
- [5] TAN L J, ZHU W, ZHOU K. Recent progress on polymer materials for additive manufacturing[J]. *Advanced Functional Materials*, 2020, 30(43): 2003062.
- [6] VELASCO-HOGAN A, XU J, MEYERS M A. Additive manufacturing as a method to design and optimize bioinspired structures[J]. *Advanced Materials*, 2018, 30(52): e1800940.
- [7] DU Shanyi. *Advanced composites and aerospace*[J]. *Acta Materiae Compositae Sinica*, 2007, 24(1): 1-12. (in Chinese)
- [8] LIU G, ZHANG X, CHEN X, et al. Additive manufacturing of structural materials[J]. *Materials Science and Engineering: R*, 2021, 145: 100596.
- [9] LOKE G, YUAN R, REIN M, et al. Structured multimaterial filaments for 3D printing of optoelectronics[J]. *Nature Communications*, 2019, 10(1): 4010.
- [10] GOH G L, ZHANG H, CHONG T H, et al. 3D printing of multilayered and multimaterial electronics: A review[J]. *Advanced Electronic Materials*, 2021, 7(10): 2100445.
- [11] YAP Y L, SING S L, YEONG W Y. A review of 3D printing processes and materials for soft robotics[J]. *Rapid Prototyping Journal*, 2020, 26(8): 1345-1361.
- [12] SACHYANI KENETH E, KAMYSHNY A, TOTARO M, et al. 3D printing materials for soft robotics[J]. *Advanced Materials*, 2020, 33(19): 2003387.
- [13] FARAHANI R D, DUBE M, THERRIAULT D. Three-dimensional printing of multifunctional nanocomposites: Manufacturing techniques and applications[J]. *Advanced Materials*, 2016, 28(28): 5794-5821.
- [14] SCHAEGLER T A, JACOBSEN A J, TORRENTS A, et al. Ultralight metallic microlattices[J]. *Science*, 2011, 334(6058): 962-965.
- [15] DIMAS L S, BRATZEL G H, EYLON I, et al. Tough composites inspired by mineralized natural materials: Computation, 3D printing, and testing[J]. *Advanced Functional Materials*, 2013, 23(36): 4629-4638.

- [16] COMPTON B G, LEWIS J A. 3D-printing of light-weight cellular composites[J]. *Advanced Materials*, 2014, 26(34): 5930-5935.
- [17] CHENG J, WANG R, SUN Z, et al. Centrifugal multimaterial 3D printing of multifunctional heterogeneous objects[J]. *Nature Communications*, 2022, 13(1): 7931.
- [18] MALEK S, GIBSON L J. Multi-scale modelling of elastic properties of balsa[J]. *International Journal of Solids and Structures*, 2017, 113/114: 118-131.
- [19] SUN C, FANG N, WU D M, et al. Projection micro-stereolithography using digital micro-mirror dynamic mask[J]. *Sensors and Actuators A: Physical*, 2005, 121(1): 113-120.
- [20] SCHMIDT M, POHLE D, RECHTENWALD T. Selective laser sintering of PEEK[J]. *CIRP Annals*, 2007, 56(1): 205-208.
- [21] ZEIN I, HUTMACHER D W, TAN K C, et al. Fused deposition modeling of novel scaffold architectures for tissue engineering applications[J]. *Biomaterials*, 2002, 23(4): 1169-1185.
- [22] HOLZMOND O, LI X. In situ real time defect detection of 3D printed parts[J]. *Additive Manufacturing*, 2017, 17: 135-142.
- [23] BAUER J, HENGSBACH S, TESARI I, et al. High-strength cellular ceramic composites with 3D microarchitecture[J]. *Proceedings of the National Academy of Sciences*, 2014, 111(7): 2453-2458.
- [24] DESHPANDE V, ASHBY M, FLECK N. Foam topology: Bending versus stretching dominated architectures[J]. *Acta Materialia*, 2001, 49(6): 1035-1040.
- [25] GAO H, JI B, JÄGER I L, et al. Materials become insensitive to flaws at nanoscale: Lessons from nature[J]. *Proceedings of the National Academy of Sciences*, 2003, 100(10): 5597-5600.
- [26] JANG D, MEZA L R, GREER F, et al. Fabrication and deformation of three-dimensional hollow ceramic nanostructures[J]. *Nature Materials*, 2013, 12(10): 893-898.
- [27] MEZA L R, DAS S, GREER J R. Strong, light-weight, and recoverable three-dimensional ceramic nanolattices[J]. *Science*, 2014, 345(6202): 1322-1326.
- [28] ZHENG X, LEE H, WEISGRABER T H, et al. Ultralight, ultrastiff mechanical metamaterials[J]. *Science*, 2014, 344(6190): 1373-1377.
- [29] MEZA L R, ZELHOFER A J, CLARKE N, et al. Resilient 3D hierarchical architected metamaterials[J]. *Proceedings of the National Academy of Sciences*, 2015, 112(37): 11502-11507.
- [30] ZHENG X, SMITH W, JACKSON J, et al. Multi-scale metallic metamaterials[J]. *Nature Materials*, 2016, 15(10): 1100-1106.
- [31] VYATSKIKH A, DELALANDE S, KUDO A, et al. Additive manufacturing of 3D nano-architected metals[J]. *Nature Communications*, 2018, 9(1): 593.
- [32] ZHANG X, VYATSKIKH A, GAO H, et al. Light-weight, flaw-tolerant, and ultrastrong nanoarchitected carbon[J]. *Proceedings of the National Academy of Sciences*, 2019, 116(14): 6665-6672.
- [33] BERGER J B, WADLEY H N, MCMEEKING R M. Mechanical metamaterials at the theoretical limit of isotropic elastic stiffness[J]. *Nature*, 2017, 543(7646): 533-537.
- [34] TANCOGNE-DEJEAN T, DIAMANTOPOULOU M, GORJI M B, et al. 3D plate-lattices: An emerging class of low-density metamaterial exhibiting optimal isotropic stiffness[J]. *Advanced Materials*, 2018, 30(45): e1803334.
- [35] DUAN S, WEN W, FANG D. Additively-manufactured anisotropic and isotropic 3D plate-lattice materials for enhanced mechanical performance: Simulations & experiments[J]. *Acta Materialia*, 2020, 199: 397-412.
- [36] ANDREW J J, VERMA P, KUMAR S. Impact behavior of nanoengineered, 3D printed plate-lattices[J]. *Materials & Design*, 2021, 202: 109516.
- [37] BONATTI C, MOHR D. Mechanical performance of additively-manufactured anisotropic and isotropic smooth shell-lattice materials: Simulations & experiments[J]. *Journal of the Mechanics and Physics of Solids*, 2019, 122: 1-26.
- [38] HAN S C, LEE J W, KANG K. A new type of low density material: Shellular[J]. *Advanced Materials*, 2015, 27(37): 5506-5511.
- [39] BONATTI C, MOHR D. Smooth-shell metamaterials of cubic symmetry: Anisotropic elasticity, yield strength and specific energy absorption[J]. *Acta Materialia*, 2019, 164: 301-321.
- [40] GUELL IZARD A, BAUER J, CROOK C, et al. Ultrahigh energy absorption multifunctional spinodal nanoarchitectures[J]. *Small*, 2019, 15(45): e1903834.
- [41] HSIEH M T, ENDO B, ZHANG Y, et al. The mechanical response of cellular materials with spinodal topologies[J]. *Journal of the Mechanics and Physics of Solids*, 2019, 125: 401-419.
- [42] SENHORA F V, SANDERS E D, PAULINO G H. Optimally-tailored spinodal architected materials for multiscale design and manufacturing[J]. *Advanced*

- Materials, 2022, 34(26): e2109304.
- [43] BARTHELAT F. Nacre from mollusk shells: A model for high-performance structural materials[J]. *Bioinspiration and Biomimetics*, 2010, 5(3): 035001.
- [44] WANG R, SUO Z, EVANS A, et al. Deformation mechanisms in nacre[J]. *Journal of Materials Research*, 2001, 16(9): 2485-2493.
- [45] ZHANG P, HEYNE M A, TO A C. Biomimetic staggered composites with highly enhanced energy dissipation: Modeling, 3D printing, and testing[J]. *Journal of the Mechanics and Physics of Solids*, 2015, 83: 285-300.
- [46] GU G X, TAKAFFOLI M, BUEHLER M J. Hierarchically enhanced impact resistance of bioinspired composites[J]. *Advanced Materials*, 2017, 29(28). DOI: 10.1002/adma.201700060.
- [47] WEAVER J C, MILLIRON G W, MISEREZ A, et al. The stomatopod dactyl club: A formidable damage-tolerant biological hammer[J]. *Science*, 2012, 336(6086): 1275-1280.
- [48] GRUNENFELDER L K, SUKSANGPANYA N, SALINAS C, et al. Bio-inspired impact-resistant composites[J]. *Acta Biomaterialia*, 2014, 10(9): 3997-4008.
- [49] NIKOLOV S, FABRITIUS H, PETROV M, et al. Robustness and optimal use of design principles of arthropod exoskeletons studied by ab initio-based multi-scale simulations[J]. *Journal of the Mechanical Behavior of Biomedical Materials*, 2011, 4(2): 129-145.
- [50] SUKSANGPANYA N, YARAGHI N A, KISAILUS D, et al. Twisting cracks in Bouligand structures[J]. *Journal of the Mechanical Behavior of Biomedical Materials*, 2017, 76: 38-57.
- [51] CHENG L, THOMAS A, GLANCEY J L, et al. Mechanical behavior of bio-inspired laminated composites[J]. *Composites Part A: Applied Science and Manufacturing*, 2011, 42(2): 211-220.
- [52] MARTIN J J, FIORE B E, ERB R M. Designing bioinspired composite reinforcement architectures via 3D magnetic printing[J]. *Nature Communications*, 2015, 6: 8641.
- [53] ZAHERI A, FENNER J S, RUSSELL B P, et al. Revealing the mechanics of helicoidal composites through additive manufacturing and beetle developmental stage analysis[J]. *Advanced Functional Materials*, 2018, 28(33): 1803073.
- [54] WU K, SONG Z, ZHANG S, et al. Discontinuous fibrous bouligand architecture enabling formidable fracture resistance with crack orientation insensitivity[J]. *Proceedings of the National Academy of Sciences*, 2020, 117(27): 15465-15472.
- [55] LIBONATI F, GU G X, QIN Z, et al. Bone-inspired materials by design: Toughness amplification observed using 3D printing and testing[J]. *Advanced Engineering Materials*, 2016, 18(8): 1354-1363.
- [56] LEI M, HAMEL C M, YUAN C, et al. 3D printed two-dimensional periodic structures with tailored in-plane dynamic responses and fracture behaviors[J]. *Composites Science and Technology*, 2018, 159: 189-198.
- [57] CLARKE D R. Interpenetrating phase composites[J]. *Journal of the American Ceramic Society*, 1992, 75(4): 739-758.
- [58] WANG L, LAU J, THOMAS E L, et al. Co-continuous composite materials for stiffness, strength, and energy dissipation[J]. *Advanced Materials*, 2011, 23(13): 1524-1529.
- [59] LI T, CHEN Y, WANG L. Enhanced fracture toughness in architected interpenetrating phase composites by 3D printing[J]. *Composites Science and Technology*, 2018, 167: 251-259.
- [60] ZHANG Y, HSIEH M T, VALDEVIT L. Mechanical performance of 3D printed interpenetrating phase composites with spinodal topologies[J]. *Composite Structures*, 2021, 263: 113693.
- [61] GIBSON L J. The hierarchical structure and mechanics of plant materials[J]. *Journal of the Royal Society Interface*, 2012, 9(76): 2749-2766.
- [62] RANEY J R, COMPTON B G, MUELLER J, et al. Rotational 3D printing of damage-tolerant composites with programmable mechanics[J]. *Proceedings of the National Academy of Sciences*, 2018, 115(6): 1198-1203.
- [63] FRANCHIN G, WAHL L, COLOMBO P. Direct ink writing of ceramic matrix composite structures[J]. *Journal of the American Ceramic Society*, 2017, 100(10): 4397-4401.
- [64] LLEWELLYN-JONES T M, DRINKWATER B W, TRASK R S. 3D printed components with ultrasonically arranged microscale structure[J]. *Smart Materials and Structures*, 2016, 25(2): 02LT01.
- [65] YANG Y, LI X, CHU M, et al. Electrically assisted 3D printing of nacre-inspired structures with self-sensing capability[J]. *Science Advances*, 2019, 5(4): eaau9490.
- [66] XU Z, HA C S, KADAM R, et al. Additive manufacturing of two-phase lightweight, stiff and high damping carbon fiber reinforced polymer microlattice

- es[J]. *Additive Manufacturing*, 2020, 32: 101106.
- [67] MATSUZAKI R, UEDA M, NAMIKI M, et al. Three-dimensional printing of continuous-fiber composites by in-nozzle impregnation[J]. *Scientific Reports*, 2016, 6: 23058.
- [68] DICKSON A N, BARRY J N, MCDONNELL K A, et al. Fabrication of continuous carbon, glass and kevlar fibre reinforced polymer composites using additive manufacturing[J]. *Additive Manufacturing*, 2017, 16: 146-152.
- [69] SUGIYAMA K, MATSUZAKI R, UEDA M, et al. 3D printing of composite sandwich structures using continuous carbon fiber and fiber tension[J]. *Composites Part A: Applied Science and Manufacturing*, 2018, 113: 114-121.
- [70] MUELLER J, RANEY J R, SHEA K, et al. Architected lattices with high stiffness and toughness via multicore-shell 3D printing[J]. *Advanced Materials*, 2018, 30(12): 1705001.
- [71] LIU Z, MEYERS M A, ZHANG Z, et al. Functional gradients and heterogeneities in biological materials: Design principles, functions, and bioinspired applications[J]. *Progress in Materials Science*, 2017, 88: 467-498.
- [72] KOKKINIS D, BOUVILLE F, STUDART A R. 3D printing of materials with tunable failure via bioinspired mechanical gradients[J]. *Advanced Materials*, 2018, 30(19): e1705808.
- [73] PHAM M S, LIU C, TODD I, et al. Damage-tolerant architected materials inspired by crystal microstructure[J]. *Nature*, 2019, 565(7739): 305-311.
- [74] VISSER C W, AMATO D N, MUELLER J, et al. Architected polymer foams via direct bubble writing[J]. *Advanced Materials*, 2019: e1904668.
- [75] MATOUŠ K, GEERS M G D, KOUZNETSOVA V G, et al. A review of predictive nonlinear theories for multiscale modeling of heterogeneous materials[J]. *Journal of Computational Physics*, 2017, 330: 192-220.
- [76] FISH J, WAGNER G J, KETEN S. Mesoscopic and multiscale modelling in materials[J]. *Nature Materials*, 2021, 20(6): 774-786.
- [77] RAJAN V P, CURTIN W A. Micromechanical design of hierarchical composites using global load sharing theory[J]. *Journal of the Mechanics and Physics of Solids*, 2016, 90: 1-17.
- [78] BENDSØE M P, KIKUCHI N. Generating optimal topologies in structural design using a homogenization method[J]. *Computer Methods in Applied Mechanics and Engineering*, 1988, 71(2): 197-224.
- [79] XIA L, BREITKOPF P. Recent advances on topology optimization of multiscale nonlinear structures[J]. *Archives of Computational Methods in Engineering*, 2016, 24(2): 227-249.
- [80] GAO J, LUO Z, LI H, et al. Topology optimization for multiscale design of porous composites with multi-domain microstructures[J]. *Computer Methods in Applied Mechanics and Engineering*, 2019, 344: 451-476.
- [81] WU Z, XIA L, WANG S, et al. Topology optimization of hierarchical lattice structures with substructuring[J]. *Computer Methods in Applied Mechanics and Engineering*, 2019, 345: 602-617.
- [82] BODDETI N, DING Z, KAIJIMA S, et al. Simultaneous digital design and additive manufacture of structures and materials[J]. *Scientific Reports*, 2018, 8(1): 15560.
- [83] BODDETI N, TANG Y, MAUTE K, et al. Optimal design and manufacture of variable stiffness laminated continuous fiber reinforced composites[J]. *Scientific Reports*, 2020, 10(1): 16507.
- [84] SANDERS E, PEREIRA A, PAULINO G. Optimal and continuous multilattice embedding[J]. *Science Advances*, 2021, 7(16): eabf4838.
- [85] CHEN C T, GU G X. Machine learning for composite materials[J]. *MRS Communications*, 2019, 9(2): 556-566.
- [86] GU G X, CHEN C T, BUEHLER M J. De novo composite design based on machine learning algorithm[J]. *Extreme Mechanics Letters*, 2018, 18: 19-28.
- [87] GU G X, CHEN C T, RICHMOND D J, et al. Bioinspired hierarchical composite design using machine learning: Simulation, additive manufacturing, and experiment[J]. *Materials Horizons*, 2018, 5(5): 939-945.
- [88] CHEN C T, GU G X. Effect of constituent materials on composite performance: Exploring design strategies via machine learning[J]. *Advanced Theory and Simulations*, 2019, 2(6): 1900056.
- [89] MA C, ZHANG Z, LUCE B, et al. Accelerated design and characterization of non-uniform cellular materials via a machine-learning based framework[J]. *NPJ Computational Materials*, 2020, 6(1): 40.
- [90] BESSA M A, GLOWACKI P, HOULDER M. Bayesian machine learning in metamaterial design: fragile becomes supercompressible[J]. *Advanced Materials*, 2019, 31(48): e1904845.
- [91] WANG Z, DABAJA R, CHEN L, et al. Machine learning unifies flexibility and efficiency of spinodal

- structure generation for stochastic biomaterial design[J]. *Scientific Reports*, 2023, 13(1): 5414.
- [92] MESSNER M C. Optimal lattice-structured materials[J]. *Journal of the Mechanics and Physics of Solids*, 2016, 96: 162-183.
- [93] GU G X, DIMAS L, QIN Z, et al. Optimization of composite fracture properties: Method, validation, and applications[J]. *Journal of Applied Mechanics*, 2016, 83(7): 071006.
- [94] GU G X, WETTERMARK S, BUEHLER M J. Algorithm-driven design of fracture resistant composite materials realized through additive manufacturing[J]. *Additive Manufacturing*, 2017, 17: 47-54.
- [95] KUMAR S, TAN S, ZHENG L, et al. Inverse-designed spinodoid metamaterials[J]. *NPJ Computational Materials*, 2020, 6(1): 73.
- [96] TUMBLESTON J R, SHIRVANYANTS D, ERMOSHIN N, et al. Continuous liquid interface production of 3D objects[J]. *Science*, 2015, 347(6228): 1349-1352.
- [97] SAJADI S M, VÁSÁRHELYI L, MOUSAVI R, et al. Damage-tolerant 3D-printed ceramics via conformal coating[J]. *Science Advances*, 2021, 7(28): eabc5028.
- [98] RASAKI S A, XIONG D, XIONG S, et al. Photopolymerization-based additive manufacturing of ceramics: A systematic review[J]. *Journal of Advanced Ceramics*, 2021, 10(3): 442-471.
- [99] CUI H, HENSLEIGH R, YAO D, et al. Three-dimensional printing of piezoelectric materials with designed anisotropy and directional response[J]. *Nature Materials*, 2019, 18(3): 234-241.
- [100] YE Yun, XIE Deqiao, JIAO Chen, et al. Study on photo-curing additive manufacturing technology of ceramic wave absorbing metamaterial structures[J]. *Journal of Nanjing University of Aeronautics and Astronautics*, 2022, 54(1): 95-102. (in Chinese)
- [101] KUANG X, ZHAO Z, CHEN K, et al. High-speed 3D printing of high-performance thermosetting polymers via two-stage curing[J]. *Macromolecular Rapid Communications*, 2018, 39(7): 1700809.
- [102] ZHANG B, KOWSARI K, SERJOUEI A, et al. Reprocessable thermosets for sustainable three-dimensional printing[J]. *Nature Communications*, 2018, 9(1): 1831.
- [103] BINYAMIN I, GROSSMAN E, GORODNITSKY M, et al. 3D printing thermally stable high-performance polymers based on a dual curing mechanism[J]. *Advanced Functional Materials*, 2023: 2214368.
- [104] BUBACK M. Free-radical polymerization up to high conversion. A general kinetic treatment[J]. *Die Makromolekulare Chemie: Macromolecular Chemistry and Physics*, 1990, 191(7): 1575-1587.
- [105] BUBACK M, HUCKESTEIN B, RUSSELL G T. Modeling of termination in intermediate and high conversion free radical polymerizations[J]. *Macromolecular Chemistry and Physics*, 1994, 195(2): 539-554.
- [106] KURDIKAR D L, PEPPAS N A J P. A kinetic study of diacrylate photopolymerizations[J]. *Polymer*, 1994, 35(5): 1004-1011.
- [107] GOODNER M D, BOWMAN C N. Development of a comprehensive free radical photopolymerization model incorporating heat and mass transfer effects in thick films[J]. *Chemical Engineering Science*, 2002, 57(5): 887-900.
- [108] FANG N, SUN C, ZHANG X. Diffusion-limited photopolymerization in scanning micro-stereolithography[J]. *Applied Physics A*, 2004, 79(8): 1839-1842.
- [109] DEWAELE M, TRUFFIER-BOUTRY D, DEVAUX J, et al. Volume contraction in photocured dental resins: The shrinkage-conversion relationship revisited[J]. *Dental Materials*, 2006, 22(4): 359-365.
- [110] LU B, XIAO P, SUN M, et al. Reducing volume shrinkage by low-temperature photopolymerization[J]. *Journal of Applied Polymer Science*, 2007, 104(2): 1126-1130.
- [111] LIU N, LIU J, LIN J, et al. Model of curing shrinkage and kinetic parameters of an acrylate-based ultraviolet-embossing resist based on free volume theory[J]. *Journal of Micro/Nanolithography, MEMS, and MOEMS*, 2013, 12(2): 023005.
- [112] LION A, HÖFER P. On the phenomenological representation of curing phenomena in continuum mechanics[J]. *Archives of Mechanics*, 2007, 59(1): 59-89.
- [113] HOSSAIN M, POSSART G, STEINMANN P. A small-strain model to simulate the curing of thermosets[J]. *Computational Mechanics*, 2008, 43(6): 769-779.
- [114] HOSSAIN M, POSSART G, STEINMANN P. A finite strain framework for the simulation of polymer curing. Part I: Elasticity[J]. *Computational Mechanics*, 2009, 44(5): 621-630.
- [115] HOSSAIN M, POSSART G, STEINMANN P. A finite strain framework for the simulation of polymer curing. Part II: Viscoelasticity and shrinkage[J]. *Computational Mechanics*, 2010, 46(3): 363-375.
- [116] HOSSAIN M, STEINMANN P. Degree of cure-dependent modelling for polymer curing processes at small-strain. Part I: Consistent reformulation[J].

- Computational Mechanics, 2013, 53(4): 777-787.
- [117] KLINGE S, BARTELS A, STEINMANN P. The multiscale approach to the curing of polymers incorporating viscous and shrinkage effects[J]. International Journal of Solids and Structures, 2012, 49(26): 3883-3900.
- [118] MERGHEIM J, POSSART G, STEINMANN P. Modeling and simulation of curing and damage in thermosetting adhesives[J]. The Journal of Adhesion, 2013, 89(2): 111-127.
- [119] MERGHEIM J, POSSART G, STEINMANN P. Modelling and computation of curing and damage of thermosets[J]. Computational Materials Science, 2012, 53(1): 359-367.
- [120] WU J, ZHAO Z, HAMEL C M, et al. Evolution of material properties during free radical photopolymerization[J]. Journal of the Mechanics and Physics of Solids, 2018, 112: 25-49.
- [121] BUGEDA G, CERVERA M, LOMBERA G, et al. Numerical analysis of stereolithography processes using the finite element method[J]. Rapid Prototyping Journal, 1995, 1(2): 13-23.
- [122] XU Y, IMAMURA M, NAKAGAWA T. Microhardness measurement of photopolymer in stereolithography[J]. Journal of Photopolymer Science and Technology, 1997, 10(2): 181-186.
- [123] HUANG Y M, JIANG C P. Curl distortion analysis during photopolymerisation of stereolithography using dynamic finite element method[J]. The International Journal of Advanced Manufacturing Technology, 2003, 21(8): 586-595.
- [124] WANG Z, LIANG H, DOBRYNIN A V. Computer simulations of continuous 3-D printing[J]. Macromolecules, 2017, 50(19): 7794-7800.
- [125] WU D, ZHAO Z, ZHANG Q, et al. Mechanics of shape distortion of DLP 3D printed structures during UV post-curing[J]. Soft Matter, 2019, 15(30): 6151-6159.
- [126] ZHANG Q, WENG S, HAMEL C M, et al. Design for the reduction of volume shrinkage-induced distortion in digital light processing 3D printing[J]. Extreme Mechanics Letters, 2021, 48: 101403.
- [127] WESTBEEK S, REMMERS J J C, VAN DOMMELEN J A W, et al. Prediction of the deformed geometry of vat photo-polymerized components using a multi-physical modeling framework[J]. Additive Manufacturing, 2021, 40: 101922.
- [128] BENNETT J. Measuring UV curing parameters of commercial photopolymers used in additive manufacturing[J]. Additive Manufacturing, 2017, 18: 203-212.
- [129] HAN W, KONG L, XU M. Advances in selective laser sintering of polymers[J]. International Journal of Extreme Manufacturing, 2022, 4(4): 042002.
- [130] BOURELL D, KRUTH J P, LEU M, et al. Materials for additive manufacturing[J]. CIRP Annals, 2017, 66(2): 659-681.
- [131] SCHMID M, AMADO A, WEGENER K. Materials perspective of polymers for additive manufacturing with selective laser sintering[J]. Journal of Materials Research, 2014, 29(17): 1824-1832.
- [132] SCHMID M, WEGENER K. Additive manufacturing: Polymers applicable for laser sintering (LS)[J]. Procedia Engineering, 2016, 149: 457-464.
- [133] REZAEI M, EBRAHIMI N G, KONTOPOULOU M. Thermal properties, rheology and sintering of ultra high molecular weight polyethylene and its composites with polyethylene terephthalate[J]. Polymer Engineering & Science, 2005, 45(5): 678-686.
- [134] KRUTH J P, MERCELIS P, VAN VAERENBERGH J, et al. Binding mechanisms in selective laser sintering and selective laser melting[J]. Rapid Prototyping Journal, 2005, 11(1): 26-36.
- [135] BALEMANS C, JAENSSON N O, HULSEN M A, et al. Temperature-dependent sintering of two viscous particles[J]. Additive Manufacturing, 2018, 24: 528-542.
- [136] CAULFIELD B, MCHUGH P E, LOHFELD S. Dependence of mechanical properties of polyamide components on build parameters in the SLS process[J]. Journal of Materials Processing Technology, 2007, 182(1/2/3): 477-488.
- [137] MOKRANE A, BOUTAOUS M H, XIN S. Process of selective laser sintering of polymer powders: Modeling, simulation, and validation[J]. Comptes Rendus Mécanique, 2018, 346(11): 1087-1103.
- [138] CHEN K, TEO H W B, RAO W, et al. Experimental and modeling investigation on the viscoelastic-viscoplastic deformation of polyamide 12 printed by multi jet fusion[J]. International Journal of Plasticity, 2021, 143: 103029.
- [139] CHILDS T, BERZINS M, RYDER G, et al. Selective laser sintering of an amorphous polymer—Simulations and experiments[J]. Proceedings of the Institution of Mechanical Engineers, Part B: Journal of Engineering Manufacture, 1999, 213(4): 333-349.
- [140] DAI K, SHAW L. Distortion minimization of laser-

- processed components through control of laser scanning patterns[J]. *Rapid Prototyping Journal*, 2002, 4(5): 270-276.
- [141] RAGHUNATH N, PANDEY P M. Improving accuracy through shrinkage modelling by using taguchi method in selective laser sintering[J]. *International Journal of Machine Tools and Manufacture*, 2007, 47(6): 985-995.
- [142] DONG L, MAKRAZI A, AHZI S, et al. Three-dimensional transient finite element analysis of the selective laser sintering process[J]. *Journal of Materials Processing Technology*, 2009, 209(2): 700-706.
- [143] PEYRE P, ROUCHAUSSE Y, DEFAUCHY D, et al. Experimental and numerical analysis of the selective laser sintering (SLS) of PA12 and PEKK semi-crystalline polymers[J]. *Journal of Materials Processing Technology*, 2015, 225: 326-336.
- [144] SHEN F, ZHU W, ZHOU K, et al. Modeling the temperature, crystallization, and residual stress for selective laser sintering of polymeric powder[J]. *Acta Mechanica*, 2021, 232(9): 3635-3653.
- [145] GREINER S, WUDY K, LANZL L, et al. Selective laser sintering of polymer blends: Bulk properties and process behavior[J]. *Polymer Testing*, 2017, 64: 136-144.
- [146] VASQUEZ G M, MAJEWSKI C E, HAWORTH B, et al. A targeted material selection process for polymers in laser sintering[J]. *Additive Manufacturing*, 2014, 1/2/3/4: 127-138.
- [147] DUPIN S, LAME O, BARRÈS C, et al. Microstructural origin of physical and mechanical properties of polyamide 12 processed by laser sintering[J]. *European Polymer Journal*, 2012, 48(9): 1611-1621.
- [148] BEAL V E, PAGGI R A, SALMORIA G V, et al. Statistical evaluation of laser energy density effect on mechanical properties of polyamide parts manufactured by selective laser sintering[J]. *Journal of Applied Polymer Science*, 2009, 113(5): 2910-2919.
- [149] GROSSKOPF A K, TRUBY R L, KIM H, et al. Viscoplastic matrix materials for embedded 3D printing[J]. *ACS Applied Materials & Interfaces*, 2018, 10(27): 23353-23361.
- [150] RANEY J R, LEWIS J A. Printing mesoscale architectures[J]. *MRS Bulletin*, 2015, 40(11): 943-950.
- [151] SEPPALA J E, HOON HAN S, HILLGARTNER K E, et al. Weld formation during material extrusion additive manufacturing[J]. *Soft Matter*, 2017, 13(38): 6761-6769.
- [152] WOOL R P, O'CONNOR K M. A theory crack healing in polymers[J]. *Journal of Applied Physics*, 1981, 52(10): 5953-5963.
- [153] KIM Y H, WOOL R P. A theory of healing at a polymer-polymer interface[J]. *Macromolecules*, 1983, 16(7): 1115-1120.
- [154] LOU R, LI H, ZHONG J, et al. A transient updated lagrangian finite element formulation for bond formation in fused deposition modeling process[J]. *Journal of the Mechanics and Physics of Solids*, 2021, 152: 104450.
- [155] WANG T M, XI J T, JIN Y. A model research for prototype warp deformation in the FDM process[J]. *The International Journal of Advanced Manufacturing Technology*, 2006, 33(11/12): 1087-1096.
- [156] ZHANG Y, CHOU Y. Three-dimensional finite element analysis simulations of the fused deposition modelling process[J]. *Proceedings of the Institution of Mechanical Engineers, Part B: Journal of Engineering Manufacture*, 2006, 220(10): 1663-1671.
- [157] ZHANG Y, CHOU K. A parametric study of part distortions in fused deposition modelling using three-dimensional finite element analysis[J]. *Proceedings of the Institution of Mechanical Engineers, Part B: Journal of Engineering Manufacture*, 2008, 222(8): 959-968.
- [158] LIU Xinhua, LI Shengpeng, LIU Zhou, et al. An investigation on distortion of PLA thin-plate part in the FDM process[J]. *The International Journal of Advanced Manufacturing Technology*, 2015, 79(5/6/7/8): 1117-1126.
- [159] ARMILLOTTA A, BELLOTTI M, CAVALLARO M. Warpage of FDM parts: Experimental tests and analytic model[J]. *Robotics and Computer-Integrated Manufacturing*, 2018, 50: 140-152.
- [160] FITZHARRIS E R, WATANABE N, ROSEN D W, et al. Effects of material properties on warpage in fused deposition modeling parts[J]. *The International Journal of Advanced Manufacturing Technology*, 2017, 95(5/6/7/8): 2059-2070.
- [161] AHN S H, MONTERO M, ODELL D, et al. Anisotropic material properties of fused deposition modeling ABS[J]. *Rapid Prototyping Journal*, 2002, 8(4): 248-257.
- [162] GARZON-HERNANDEZ S, ARIAS A, GARCIA-GONZALEZ D. A continuum constitutive model for FDM 3D printed thermoplastics[J]. *Composites Part B: Engineering*, 2020, 201: 108373.
- [163] MIRZENDEHDEL A M, RANKOUHI B,

- SURESH K. Strength-based topology optimization for anisotropic parts[J]. *Additive Manufacturing*, 2018, 19: 104-113.
- [164] BARTOLAI J, SIMPSON T W, XIE R. Predicting strength of additively manufactured thermoplastic polymer parts produced using material extrusion[J]. *Rapid Prototyping Journal*, 2018, 24(2): 321-332.
- [165] JIN Z, ZHANG Z, GU G X. Autonomous in-situ correction of fused deposition modeling printers using computer vision and deep learning[J]. *Manufacturing Letters*, 2019, 22: 11-15.
- [166] JIN Z, ZHANG Z, GU G X. Automated real-time detection and prediction of interlayer imperfections in additive manufacturing processes using artificial intelligence[J]. *Advanced Intelligent Systems*, 2019, 2(1): 1900130.
- [167] THOMPSON A, MASKERY I, LEACH R K. X-ray computed tomography for additive manufacturing: A review[J]. *Measurement Science and Technology*, 2016, 27(7): 072001.
- [168] CAO X, JIANG Y, ZHAO T, et al. Compression experiment and numerical evaluation on mechanical responses of the lattice structures with stochastic geometric defects originated from additive-manufacturing[J]. *Composites Part B: Engineering*, 2020, 194: 108030.
- [169] GENG L, WU W, SUN L, et al. Damage characterizations and simulation of selective laser melting fabricated 3D reentrant lattices based on in-situ CT testing and geometric reconstruction[J]. *International Journal of Mechanical Sciences*, 2019, 157: 231-242.
- [170] CAO X, HUANG Z, HE C, et al. In-situ synchrotron X-ray tomography investigation of the imperfect smooth-shell cylinder structure[J]. *Composite Structures*, 2021, 267: 113926.
- [171] HURLEY R C, PAGAN D C. An in-situ study of stress evolution and fracture growth during compression of concrete[J]. *International Journal of Solids and Structures*, 2019, 168: 26-40.
- [172] GARCEA S C, WANG Y, WITHERS P J. X-ray computed tomography of polymer composites[J]. *Composites Science and Technology*, 2018, 156: 305-319.
- [173] BALE H A, HABOUB A, MACDOWELL A A, et al. Real-time quantitative imaging of failure events in materials under load at temperatures above 1 600 °C[J]. *Nature Materials*, 2013, 12(1): 40-46.
- [174] CHEN Y, PENG X, KONG L, et al. Defect inspection technologies for additive manufacturing[J]. *International Journal of Extreme Manufacturing*, 2021, 3(2): 022002.
- [175] SHAIKEEA A J D, CUI H, O' MASTA M, et al. The toughness of mechanical metamaterials[J]. *Nature Materials*, 2022, 21(3): 297-304.
- [176] YANG T, JIA Z, CHEN H, et al. Mechanical design of the highly porous cuttlebone: A bioceramic hard buoyancy tank for cuttlefish[J]. *Proceedings of the National Academy of Sciences*, 2020, 117(38): 23450-23459.
- [177] YANG T, CHEN H, JIA Z, et al. A damage-tolerant, dual-scale, single-crystalline microlattice in the knobby starfish, *protoreaster nodosus*[J]. *Science*, 2022, 375(6581): 647-652.
- [178] NIE Yinghao, CHENG Gengdong, LI Zheng. Study on clustering finite element analysis for predicting the effective properties of composite materials and the properties of interaction matrix[J]. *Journal of Dalian University of Technology/Dalian Ligong Daxue Xuebao*, 2020, 60(5): 441-445. (in Chinese)

Acknowledgements This work was supported by the National Natural Science Foundation of China (No.12202190), Outstanding Postdoctoral Program in Jiangsu Province (No. 2022ZB233), and Research Start-up Funding from Nanjing University of Aeronautics and Astronautics (No.90YAH21131).

Author Dr. ZHANG Qiang obtained his Ph.D. degree in solid mechanics from the Department of Mechanics and Engineering Sciences, Peking University, in 2021. From 2018 to 2020, he worked as a visiting scholar at Georgia Institute of Technology. He joined Nanjing University of Aeronautics and Astronautics in 2021 and he is currently an assistant professor of College of Aerospace Engineering. His research interests include mechanism of formation and evolution of biological structures, advanced 3D printing techniques, and mechanics of 3D-printed materials.

Author contributions Dr. ZHANG Qiang designed the study and wrote the manuscript. Prof. SHI Yan and Prof. GAO Cunfa contributed to the discussion and background of the study. All authors commented on the manuscript draft and approved the submission.

Competing interests The authors declare no competing interests.

多组分多层次3D打印材料研究进展

张 强, 师 岩, 高存法

(南京航空航天大学航空航天结构力学及控制全国重点实验室, 南京 210016, 中国)

摘要:多组分多层次3D打印材料(McM13DPMs)是一种新兴的先进材料,源于多孔材料、复合材料和增材制造的融合。由于增材制造赋予了McM13DPMs三维架构跨越广泛组分构成和结构类型的能力,McM13DPMs拥有杰出的机械性能,甚至是通常被认为相互排斥的性能(例如高强度和高韧性)。本文重点介绍为了实现高性能结构用McM13DPMs所必须解决的科学挑战以及最近研究工作对此做出的努力,将从结构设计、制造过程建模、缺陷表征和性能评价3个方面对相关案例进行回顾。最后,本文指出了当前研究的不足之处,并展望了McM13DPMs的未来发展,包括讨论了进一步推进这一新兴领域发展的几个可能的研究方向。

关键词:多组分多层次3D打印材料;结构设计;制造过程建模;缺陷表征和性能评价